UNIVERSIDADE FEDERAL DE SANTA CATARINA
CENTRO DE CIÊNCIAS DA SAÚDE
PROGRAMA DE PÓS-GRADUAÇÃO EM ODONTOLOGIA

ANÁLISE POR ELEMENTOS FINITOS DA ESTIMULAÇÃO ELÉTRICA NA OSSEOINTEGRAÇÃO DOS IMPLANTES DENTAIS DE TITÂNIO

DOUTORADO

Letícia Moro Bins Ely

Florianópolis
2018

UNIVERSIDADE FEDERAL DE SANTA CATARINA
PROGRAMA DE PÓS-GRADUAÇÃO EM ODONTOLOGIA

Letícia Moro Bins Ely

ANÁLISE POR ELEMENTOS FINITOS DA ESTIMULAÇÃO ELÉTRICA NA OSSEOINTEGRAÇÃO DOS IMPLANTES DENTAIS DE TITÂNIO

Tese de doutorado submetida ao Programa de Pós-graduação em Odontologia da Universidade Federal de Santa Catarina para obtenção do título de Doutor em Odontologia.

Orientador: Prof. Dr. César Augusto Magalhães Benfatti
Coorientador: Prof. Dr. Júlio César Matias de Souza

Área de concentração: Implantodontia.

Florianópolis
2018

Ficha de identificação da obra elaborada pelo autor,
através do Programa de Geração Automática da Biblioteca Universitária da UFSC.

Moro Bins Ely, Letícia
ANÁLISE POR ELEMENTOS FINITOS DA ESTIMULAÇÃO ELÉTRICA NA OSSEOINTEGRAÇÃO DOS IMPLANTES DENTAIS DE TITÂNIO / Letícia Moro Bins Ely ; orientador, César Augusto Magalhães Benfatti , coorientador, Júlio César Matias de Souza , 2018.
95 p.

Tese (doutorado) - Universidade Federal de Santa Catarina, Centro de Ciências da Saúde, Programa de Pós-Graduação em Odontologia, Florianópolis, 2018.

Inclui referências.

1. Odontologia. 2. Elemento finito. 3. Terapia de estimulação elétrica. 4. Titânio. 5. Implante dental. I. Augusto Magalhães Benfatti , César . II. César Matias de Souza , Júlio . III. Universidade Federal de Santa Catarina. Programa de Pós-Graduação em Odontologia. IV. Título.

Letícia Moro Bins Ely

ANÁLISE POR ELEMENTOS FINITOS DA ESTIMULAÇÃO ELÉTRICA NA OSSEOINTEGRAÇÃO DOS IMPLANTES DENTAIS DE TITÂNIO

DOUTORADO EM ODONTOLOGIA

E aprovado em 01 de outubro de 2018, atendendo as normas da legislação vigente da Universidade Federal de Santa Catarina, Programa de Pós-Graduação em Odontologia. Área de Concentração: **Implantodontia**

Às pessoas que amo...

AGRADECIMENTOS

Agradeço a Deus, por ser a razão de tudo.

À minha família, pelo exemplo de vida, amor e carinho.

À minha avó Maria Beatriz, por ser modelo de vocação docente e por acreditar no meu potencial.

Aos meus pais, Jorge e Vera Helena, pelo incentivo à vida acadêmica e, sobretudo, por me ensinarem a sonhar, a acreditar e a buscar.

Ao meu marido Luis Paulo, por ser paciente, companheiro, amigo e carinhoso. Seu abraço é o melhor lugar do mundo. Obrigada a toda sua família pelo apoio, especialmente à dona Lucila e ao Seu Sírio.

À Helena Maria de Araújo, por acreditar no meu potencial. Sua dedicação à Odontologia fez eu me apaixonar por esta profissão.

Aos amigos que conquistei durante a vida, especialmente àqueles que me apoiaram nessa caminhada.

Ao Prof. Dr. César Benfatti, pela orientação e colaboração para o meu desenvolvimento acadêmico e profissional. Sua forma leve de ver a vida, me inspira.

Ao Prof. Dr. Ricardo Magini, pela confiança e disponibilidade. Seu amor à vida acadêmica é fonte de inspiração e motivação.

Ao Prof. Dr. Júlio Souza, pela confiança, disponibilidade e apoio para realização desse trabalho.

À Prof. Dr.ª Daniela Suzuki, pela disponibilidade, realização dos experimentos e, especialmente, pela motivação e pelas conversas.

Ao Prof. Dr. Bruno Henriques, pela disponibilidade e colaboração.

Aos Professores do CEPID/UFSC: Antônio Carlos Car
Marco Aurélio Bianchini, Cláudia Volpato, Ariadne da Cruz,
ensinamentos e experiências transmitidos.

Aos Professores da UFSC: Sônia Probst, Almir Spinelli e Luismar Porto, pelo apoio e ensinamentos.

Aos colegas do curso de Mestrado e Doutorado do CEPID, pela amizade e conhecimentos transmitidos.

Aos funcionários da UFSC, especialmente à Silvane, pela dedicação e colaboração.

Aos pacientes, pela confiança e paciência.

Ao Programa de Pós-Graduação em Odontologia e à UFSC, pela acolhida nos últimos anos.

Ao CNPq e à CAPES pelo apoio financeiro.

"*A persistência é o caminho do êxito"*
Charles Chaplin

RESUMO

Estudos experimentais demonstraram que a estimulação elétrica promove a osteogênese e proporciona maior área de contato osso-implante (BIC). Estudo *in vivo* (Bins-Ely et al., 2017) revelou os maiores valores médios de contato osso-implante (82%) quando submetidos à aplicação de corrente elétrica de 20 μA. Considerando-se vários fatores que afetam o processo de osseointegração, análises de elementos finitos também podem ser uma boa estratégia para distinguir preliminarmente aspectos chave para melhorar a osseointegração dos implantes. O objetivo deste estudo foi avaliar a influência de diferentes densidades e amplitudes de corrente elétrica na porcentagem de contato osso-implante utilizando o método dos elementos finitos. A distribuição do campo elétrico no tecido biológico foi calculada pelo método dos elementos finitos (FEM) usando o COMSOL Multiphysics® (Estocolmo, Suécia) e os cálculos do modelo 3D foram executados em um computador pessoal. Modelos numéricos foram realizados em implantes de grau IV de titânio comercialmente puros conectados a uma bateria de 1,5 V com resistência elétrica (R) a 150 kΩ em 10 μA ou a 75 kΩ em 20 μA. A porcentagem de BIC simulado foi analisada variando-se a corrente elétrica de 1 a 60 μA e a condutividade elétrica da interface osso-implante ($_{BC+TiO2}$) foi de 0,30 S/m. A variação da aplicação de corrente elétrica foi simulada para regiões peri-implantar cervicais e apicais. No entanto, a aplicação de corrente elétrica foi realizada na região peri-implantar apical e apresentou um BIC de 79% para aplicação de 20 μA; 93% para aplicação de 30 μA e 98% para aplicação de 40 μA. Por outro lado, a aplicação de corrente elétrica foi realizada na região peri-implantar cervical e apresentou menor BIC (%) para toda a fonte de corrente aplicada. Uma fonte de corrente elétrica abaixo de 10 μA não foi suficiente para aumentar os valores médios de BIC. No entanto, fontes de corrente elétrica variando de 10 a 20 μA aumentaram os valores de BIC até cerca de 60%, enquanto uma fonte elétrica a 30-40 μA resultou em valores de BIC em cerca de 90%. O posicionamento da fonte de corrente elétrica pode influenciar os valores de BIC, uma vez que o posicionamento da fonte elétrica próxima ao ápice do implante apresentou os maiores valores de BIC quando comparados àqueles registrados na região coronal do implante

Palavras-chave: Elemento finito, Terapia de estimulação elétrica, Titânio, Implante dental.

ABSTRACT

Experimental studies have shown that electrical stimulation promotes osteogenesis and provides higher contact area of bone/implant interface (BIC). An in vivo study (Bins-Ely at al., 2017) revealed the highest mean values of bone-implant contact (82%) when submitted to 20 μA electrical current application. Considering several factors that affect the osseointegration process, finite element analyses can also be a good strategy to preliminary distinguish key aspects to enhance implants osseointegration. The aim of this study was to evaluate the influence of different density and amplitude of electric current on the percentage of bone-implant contact using the finite element method. The electric field distribution on biological tissue was computed by finite element method (FEM) using the COMSOL Multiphysics® (Stockholm, Sweden) and the *3D* model calculations were run on a personal computer. Numerical models were performed on commercially pure titanium grade IV implants connected to a 1.5 V battery with an electrical resistance (*R*) at 150 kΩ on 10 μA or at 75 kΩ on 20 μA. The percentage of simulated BIC was analyzed by varying the electric current from 1 up to 60 μA and the electrical conductivity of the interface implant-bone ($_{BC+TiO2}$) was 0.30 S/m. The variation of electric current application was simulated for cervical and apical peri-implant regions. However, electrical current application was performed at the apical peri-implant region and showed a BIC of 79% for application of 20 μA; 93% for application of 30 μA and 98% for application of 40 μA. On the other hand, electrical current application was performed at cervical peri-implant region and showed lower BIC (%) for all current source applied. Conclusion: An electrical current source below 10 μA was not enough to increase the BIC mean values. However, electrical current sources ranging from 10 up to 20 μA increased the BIC values up to around 60% while an electrical source at 30-40 μA resulted in BIC values at about 90%. The positioning of the electrical current source can influence the BIC values once the electrical source positioning close to the implant apex showed the highest BIC values when compared to those recorded at the coronal region of the implant

Keywords: Finite element, Electric stimulation therapy, Titanium, Dental implants.

LISTA DE FIGURAS

Figura 1. Ilustração esquemática da geometria do implante-bateria. O desenho de seção cruzada revela o *design* interno do implante conectado à bateria. Distância (h); fluxo de corrente elétrica (I); resistência elétrica (*R*) e implante dentário de titânio (Ti).....40

Figura 2. Esquema do implante e região ao redor dos tecidos peri-implantares. (A) Interface implante-osso é detalhada de acordo com estudos anteriores [49], sendo resistência elétrica (*R*) e implante dentário de titânio (Ti). (B) Circuito elétrico equivalente do implante dentário e tecidos adjacentes, onde a corrente elétrica total (I_T) flui no implante dentário e tecidos circundantes (Ti); resistência elétrica do titânio (R_{Ti}); resistência do TiO_2 e coágulo sanguíneo (BC) (R_{TiO2}); resistência óssea esponjosa e cortical (R_B) e resistência dos tecidos moles (R_S).....42

Figura 3. Condutividade elétrica da região do coágulo sanguíneo. A seta delimita as variações experimentais dos resultados do BIC (%) para 10 µA obtidos por [33].....44

Figura 4. Distribuição da densidade de corrente no implante para (A, C) 10 µA e (B, D) 20 µA. $\sigma_{BC+TiO2}$= = 0,3 S / m. (C, D) A interface de implante ósseo mostrada em detalhes. A cor preta indicava J <0,01 A / m2 enquanto a cor do arco-íris estava em 0,01 A / m2 <J <0,5 A / m2, e branca a J> 0,5 A / m2.....45

Figura 5. Influência da variação atual da fonte na porcentagem de contato osso-implante (BIC). $\sigma_{BC+TiO2}$= = 0,3 S / m. h = 10 mm, corrente aplicada na região peri-implantar apical.....46

Figura 6. Influência da variação atual da fonte na porcentagem de contato osso-implante (BIC). $\sigma_{BC+TiO2}$= = 0,3 S / m. h = 5 mm, corrente aplicada na região peri-implantar cervical.....46

LISTA DE TABELAS

Tabela 1. Propriedades dielétricas dos materiais e dos tecidos envolvidos no estudo……41

SIGLAS, SÍMBOLOS E ABREVIATURAS

A	Ampère
A/m^2	Ampère por metro quadrado
A	Área
BC	Blood clot (coágulo)
BIC	Bone-implant contact (contato osso-implante)
C	Capacitância
q	Carga elétrica
l	Comprimento
G	Condutância
σ	Condutividade elétrica
($\sigma_{BC+TiO2}$)	Condutividade elétrica
k	Constante dielétrica
CA	Corrente alternada
CD	Corrente direta
CC	Corrente contínua
C	Coulombs
C/s	Coulombs por segundo
J	Densidade de corrente
TiO_2	Dióxido de titânio
DC	Direct current
h	Distância
EF ou E	Electric field
w	Energia
EC	Estímulo capacitivo
EI	Estímulo indutivo
F	Farad
I	Fluxo de corrente elétrica contínua
I_T	Fluxo de corrente elétrica total
FDA	Food and Drug Administration
Ti	Implante dentário de titânio
i	Intensidade de corrente elétrica
Δt	Intervalo de tempo
$(\Omega\text{-m})^{-1}$	Inverso de ohm/metro
J	Jaules
kΩ	KiloOhm
FEM	Método de elementos finitos
m^2	Metro quadrado
µA	Microampère

$\mu A/cm^2$	Microampère por centímetro quadrado
µm	Micrometro
mA/m^2	Miliampère por metro quadrado
mm	Milímetro
mm	Milímetro
mm	Milímetro
Ω	Ohms
ε_r	Permissividade relativa
pH	Potencial hidrogeniônico
R	Resistência elétrica
R_{Ti}	Resistência elétrica do Cp Ti
R_S	Resistência elétrica do tecido mole
R_{TiO2}	Resistência elétrica do TiO_2 + BC
R_B	Resistência elétrica óssea (cortical + medular)
ρ	Resistividade elétrica
SLA	Sandblasted and acid aching surfaces
s	Segundos
S	Siemens
S/m	Siemens por metro
v	Tensão
Cp Ti	Titânio comercialmente puro
Ti-CP	Titânio puro
V	Volts

SUMÁRIO

1 INTRODUÇÃO 25

2 PERGUNTAS DE PESQUISA 31

2.1 PERGUNTA PRINCIPAL 31
2.2 PERGUNTAS SECUNDÁRIAS 31

3 JUSTIFICATIVA 33

4 OBJETIVOS 35

4.1 OBJETIVO GERAL 35
4.2 OBJETIVOS ESPECÍFICOS 35

5 ARTIGO EM INGLÊS 37

5.1 ABSTRACT 37
5.2 INTRODUCTION 37
5.3 MATERIAL AND METHODS 40
5.3.1 Numerical model of the implant-battery-bone assembly 40
5.3.2 Finite element analysis 42
5.3.3 Parameters models 43
5.4 RESULTS 43
5.5 DISCUSSION 47
5.6 CONCLUSIONS 50
5.7 REFERENCES 51

6 METODOLOGIA EXPANDIDA 59

6.1 CONCEITOS BÁSICOS EM ELETROQUÍMICA 59
6.1.1 Piezoeletricidade e Lei de Wolff 59
6.1.2 Fundamentos de Circuitos Elétricos 59
6.2 SIMULAÇÃO NUMÉRICA 63
6.2.1 Aquisição dos dados e descrição do modelo 63
6.2.2 Modelagem numérica 64
6.2.3 Parâmetros da simulação 65

7 REFERÊNCIAS 67

8 APÊNDICE 73

9 ANEXO 79

1 INTRODUÇÃO

A terapia com implantes dentários para substituir um ou mais dentes em pacientes parcial ou totalmente desdentados tornou-se uma técnica bem documentada e cientificamente aceita (ELIAS et al., 2008). Para que o implante dentário seja funcional é necessário haver osseointegração, definida como a formação de uma interface direta entre implante e osso sem interposição de tecidos moles à microscopia óptica (BRÅNEMARK PI, HANSSON BO, ADELL R, BREINE U, LINDSTRÖM J, HALLÉN O, 1977).

O titânio, comercialmente puro ou suas ligas, é largamente aplicado na confecção de implantes dentários, pois apresenta alta resistência à corrosão e ótima biocompatibilidade, devido à formação de uma fina camada de óxido de titânio (TiO_2) (LIU; CHU; DING, 2004; STEINEMANN, 1998).

Nos últimos anos, acadêmicos e pesquisadores têm desenvolvido diferentes topografias de superfícies e formas geométricas de sistemas de implantes dentários com objetivo de permitir aos clínicos a reabilitação oral em tempo mínimo (BAGGI et al., 2008; COELHO et al., 2015). A compreensão da influência das características superficiais dos materiais na biocompatibilidade e no processo de osseointegração tem sido particularmente importante para o sucesso clínico dos implantes (BROGGINI et al., 2006; CRUZ et al., 2011; QUIRYNEN; DE SOETE; VAN STEENBERGHE, 2002; TEUGHELS et al., 2006). Consequentemente, a taxa de sucesso é de aproximadamente 89% após 10 a 15 anos de acompanhamento e está diretamente relacionada, não somente ao processo de osseointegração da superfície do implante, mas também, com a estabilidade da interface implante-osso a longo prazo (ALBREKTSSON et al., 1981; LIMA et al., 2006; ROOS-JANSAKER et al., 2006).

Assim, considera-se que a superfície do implante é fundamental para alcançar e sustentar os resultados estéticos, pois a manutenção óssea contribui para a altura e volume do tecido mole adequados, levando a resultados estéticos aprimorados. Para este fim, a seleção de um sistema de implante com uma superfície projetada para melhorar a osseointegração, preservar o tecido ósseo e fornecer proteção contra o desenvolvimento de peri-implantite é de grande importância (LAZZARA, 2012).

Um implante com uma microtopografia de superfície complexa é essencial tanto para a promoção de osteogênese de contato, quanto para

adesão da matriz óssea à superfície. Esses fenômenos mostram a importância e a influência que a microtopografia da superfície do implante tem na cicatrização precoce e na otimização das respostas biológicas durante o processo de cicatrização (SEZIN; CROHARÉ; IBANEZ, 2016).

O uso de titânio e suas ligas, em implantes dentários, marca uma era em que um dos principais objetivos tem sido a redução ou eliminação do *gap* entre o procedimento cirúrgico e a carga funcional devido à melhor resposta do hospedeiro ao implante (VERVAEKE; COLLAERT; DE BRUYN, 2013). Na década de 80, os implantes utilizados apresentavam superfície lisa e permaneciam submersos por um período médio de 6 meses para permitir a osseointegração e, consequente, função. Hoje, implantes com diferentes micro e macro geometrias reduziram o tempo de espera e, em casos selecionados, permitem a restauração imediata da função e da estética (WEBER et al., 2009).

A fim de aprimorar o comportamento dos biomateriais metálicos, sua biocompatibilidade e também as suas propriedades mecânicas e físico-químicas, muitos estudos têm priorizado o conhecimento e aperfeiçoamento dos tratamentos de superfície (BORDJI et al., 1996; BUSER et al., 1991; COELHO et al., 2015; HU; YANG, 2014; PONSONNET et al., 2003; SELA et al., 2007; THOMAS; COOK, 1985).

Segundo Duan and Wang (DUAN; WANG, 2006), os métodos de modificação de superfície podem ser classificados nas seguintes categorias: 1) adição de materiais de funções desejáveis à superfície, 2) conversão da superfície existente em composições e / ou topografias mais desejáveis, 3) remoção de material da superfície existente para criar topografias. As três categorias de modificação podem ser alcançadas por diferentes técnicas, dependendo das aplicações, entre elas: técnicas físicas como revestimento por plasma spray, deposição física de vapor (categoria 1), implantação de íons (categoria 2), usinagem de superfície e jateamento (categoria 3). Ou por técnicas químicas, como a deposição biomimética de revestimentos de fosfato de cálcio, imobilização de superfície de moléculas funcionais (categoria 1), oxidações eletroquímicas (categoria 2) e corrosões ácidas (categoria 3).

Além da rugosidade de superfície, a química é uma variável importante para aposição óssea peri-implantar, porque influencia a carga de superfície e a molhabilidade (KILPADI; LEMONS, 1994). A energia de superfície desempenha um papel essencial na adesão dos osteoclastos, enquanto sua dispersão é dependente da química da

superfície, especialmente na adsorção de proteínas e nas camadas de apatita recém-formadas. Assim, a adesão e dispersão celular são significativamente maiores em superfícies hidrofílicas do que em superfícies hidrofóbicas (PONSONNET et al., 2003).

A molhabilidade da superfície do biomaterial controlará as proteínas capazes de adsorver na superfície e a formação do coágulo sanguíneo e da rede de fibrina (KOPF et al., 2015). A combinação de aumento da rugosidade superficial e hidrofilia pode interagir sinergicamente para produzir um microambiente adequado para reduzir o tempo de cicatrização e aumentar a osseointegração, o que pode elevar as taxas de sucesso dos implantes (HOTCHKISS et al., 2016).

Com a finalidade de acelerar o processo de osseointegração, existem alternativas biofísicas, como mecânica, sonora e elétrica, além das terapias bioquímicas osteoindutoras (AARON et al., 2006). Os primeiros estudos sobre o efeito do estresse ou deformação nas propriedades elétricas do osso mostraram que o estresse de compressão causa um potencial negativo entre os eletrodos inseridos, o que leva à reabsorção óssea, enquanto a tensão de tração gera um potencial positivo, causando o crescimento ósseo (BASSETT; PAWLUK; PILLA, 1974; FUKADA; YASUDA, 1957). Esses resultados levaram ao desenvolvimento de diferentes métodos para a estimulação elétrica do osso. O método invasivo, e mais comumente usado, é o estímulo de corrente contínua (CC). Por outro lado, as formas não invasivas de estimular o crescimento ósseo são: estímulo indutivo (EI) e estímulo capacitivo (EC) (COCHRAN, 1972). O uso de CC foi aprovado pela *Food and Drug Administration* (FDA) em 1979 e tem sido usado clinicamente por mais de 36 anos para a cura de fraturas (NELSON et al., 2003).

Estudos prévios in vitro mostraram que a estimulação elétrica, seja por CC, gerando campo elétrico (EI) ou EC, melhora a cicatrização óssea (BUCH; ALBREKTSSON; HERBST, 1984), a proliferação celular (ARO et al., 1984) e a síntese de matriz extracelular (FRIEDENBERG et al., 1989). Estudos in vivo também mostraram que a estimulação elétrica promove a osteogênese (SHIGINO et al., 2001) e proporciona maior área de contato da interface osso / implante (BINSELY et al., 2017; SHAFER et al., 1995; SHAYESTEH et al., 2007; SONG et al., 2009). De acordo com Shafer et al. (SHAFER et al., 1995), a aplicação de baixa intensidade de corrente elétrica (7,5 μA) não tem efeito positivo na consolidação óssea. E, apesar de apresentar relatos de sucesso clínico (BRIGHTON et al., 1977; KLECZYNSKI, 1988) na literatura, o mecanismo subjacente pelo qual ocorre a osteogênese,

induzida eletricamente, ainda não está claro. Não há consenso na literatura sobre os princípios operacionais de ambas as densidades de corrente elétrica 0,01 A/m^2 <J <0,5 A/m^2 (GITTENS et al., 2011) e amplitudes 7 μA a 50 μA (NELSON et al., 2003) aplicadas na interface osso-implante.

Estudo clínico realizado na área ortopédica, acredita que as terapias externas, como estimulação elétrica, aumentam a consolidação óssea e a reparação de fraturas com uma taxa de sucesso de 80 a 85% em fraturas não consolidadas agravadas por características biológicas locais inadequadas e fatores sistêmicos, por exemplo, tabagismo, diabetes e alguns medicamentos (antiinflamatórios não esteróides e esteróides) (VERDONK et al., 2015). Por tanto, a estimulação elétrica tem caráter coadjuvante no tratamento de complicações relacionadas à cicatrização óssea, especialmente em pacientes de alto risco (COOK; SUMMERS; COOK, 2015). No entanto, é necessário investigação adicional e desenhos de estudo de alta qualidade para determinar as modalidades de tratamento mais eficazes e as patologias mais utilizadas com a estimulação óssea.

Bins-Ely et al. (BINS-ELY et al., 2017) avaliaram, por estudo histomorfométrico, a influência da aplicação de corrente elétrica em implantes de titânio estimulando a formação óssea. Implantes com superfície usinada foram comparados com implantes após aplicação de corrente elétrica direta e contínua de 10 μA e 20 μA por 7 e 14 dias. Após 7 dias de estimulação elétrica, não foram observadas diferenças estatísticas na área de contato da interface osso-implante. Por outro lado, implantes de titânio submetidos a 20 μA de corrente elétrica por 14 dias apresentaram melhor aposição óssea na superfície do implante com 82% de BIC e 44 μm na área periférica ($p < 0,01$). Não houve diferença estatística entre os grupos 10 μA e controle ($p > 0,05$). Os autores concluíram que existe uma correlação positiva entre a porcentagem de contato osso-implante e a aplicação de corrente elétrica de 20 μA. No entanto, este estudo foi realizado em tíbia de cão e avaliado por curtos períodos de cicatrização.

Considerando-se a importância das mudanças na superfície dos implantes de titânio na qualidade e sucesso da osseointegração e a pouca compreensão do efeito da estimulação elétrica do titânio, as simulações numéricas que predizem ou confirmam esses achados experimentais são uma importante ferramenta para o planejamento do tratamento da aplicação elétrica. Desta forma, é possível avaliar diferentes parâmetros separadamente, levando a um planejamento adequado de estudos *in vitro* e *in vivo*.

O objetivo deste estudo foi avaliar a influência de diferentes densidades e amplitudes de corrente elétrica na porcentagem de contato osso-implante utilizando o método dos elementos finitos. Para isso, os resultados histomorfométricos encontrados no estudo de Bins-Ely et al. (BINS-ELY et al., 2017), em modelo animal, foram utilizados como referência. Este estudo numérico foi realizado levando em conta a interface osso-implante e a presença de coágulo sanguíneo.

A hipótese nula deste estudo foi que a aplicação de corrente elétrica ideal é de cerca de 20 μA e que a posição da fonte de corrente dentro do implante influencia a área do BIC.

2 PERGUNTAS DE PESQUISA

2.1 PERGUNTA PRINCIPAL

Qual a influência de diferentes densidades e amplitudes de corrente elétrica na porcentagem de contato osso-implante?

2.2 PERGUNTAS SECUNDÁRIAS

- Qual a faixa de densidade e amplitude de aplicação ideal?
- Aplicação de corrente elétrica pode causar necrose tecidual?
- A posição da fonte de corrente elétrica dentro do implante influencia a área de contato osso-implante?

3 JUSTIFICATIVA

Dado aos resultados positivos de pesquisas realizadas pelo grupo de pesquisadores do Centro de Estudos e Pesquisa em Implantes Dentários (CEPID) ao avaliar a influência de estímulos elétricos na osseintegração de implantes de titânio, instalados em tíbia de cães, assim como aos resultados positivos encontrados na literatura, tanto em estudos clínicos quando em estudos experimentais (*in vivo* e *in vitro)* surge a curiosidade de avaliar a influência de diferentes densidades e amperagens de corrente elétrica. Além disso, há a necessidade de padronização dos dados e entendimento do processo de osteogênese durante o estímulo de corrente elétrica.

Entretanto, por uma questão ética, utiliza-se cada vez menos estudos experimentais *in vivo*, sendo a simulação numérica (experimentos *in sílico*) uma forma vantajosa de apresentar respostas sobre a influência de diferentes densidades e amplitudes de aplicação e da posição da fonte da corrente elétrica na porcentagem de contato osso-implante.

4 OBJETIVOS

4.1 OBJETIVO GERAL

Avaliar a influência de diferentes densidades e amplitudes de corrente elétrica na porcentagem de contato osso-implante utilizando modelo matemático.

4.2 OBJETIVOS ESPECÍFICOS

- Definir qual a faixa de densidade e amplitude ideal de corrente elétrica para aumentar a porcentagem de contato osso-implante;
- Verificar qual a faixa de densidade e amplitude não causam alterações na porcentagem de contato osso implante;
- Observar se a aplicação de densidade e amplitude de corrente elétrica pode causar necrose na interface osso-implante;
- Verificar se a posição da fonte de corrente dentro do implante influencia a área de contato osso-implante.

5 ARTIGO EM INGLÊS

NUMERICAL MODELLING THE ELECTRICAL STIMULATION ON IMPLANT OSSEOINTEGRATION

5.1 ABSTRACT

The aim of this study was to evaluate the influence of different density and amplitude of electric current on the percentage of bone-implant contact (BIC) using the finite element method. Numerical models were performed on commercially pure titanium grade IV implants connected to a 1.5 V battery with an electrical resistance (*R*) at 150 kΩ on 10 μA or at 75 kΩ on 20 μA. The percentage of simulated BIC was analysed by varying the electric current from 1 up to 60 μA. The variation of electric current application was simulated for coronal and apical peri-implant regions. The findings showed that a source applying a direct and constant electric current below 10 μA cannot provide acceptable current density for osseointegration (BIC < 55%). However, current sources from 10 to 20 μA or 30 to 40 μA resulted in BIC above 60 and 90%, respectively. The application of the current source at the apical peri-implant region resulted in the highest BIC percentage at around 86.1%. Although the model is a simplified version of the biological process in the bone-implant interface, the findings obtained in this study can predict a magnitude of electrical current density required to stimulate osseointegration. The location and intensity of the electrical current source can increase the resultant electrical current density at the implant-bone and enhance the bone healing process.

Keywords: Finite element, Electric stimulation therapy, Titanium, Dental implants.

5.2 INTRODUCTION

Since the 1970s, titanium-based implants have been widely used in dentistry due to their physicochemical and biological behavior to establish a direct contact with the surrounding bone (1). Conventional loading - at least three months in the mandible and six months in the maxilla - (2) it has been recommended to minimize the risk of soft tissue encapsulation, consequent loss of osseointegration and implant failure (1). Although 10-year implant survival rate of 99.7% (3), recent studies have pursued to decrease the bone healing period (4). In fact, peculiar

clinical conditions can occur such as the placement of implants in regions with poor bone quality and volume (5). Also, bone grafts and bio-absorbable membranes are often required for vertical and horizontal bone augmentation (6). Factors related to the patients, prosthetic, and surgical conditions statistically affect implant failure rates (7). Thus, shorten the healing time can avoid early risks of failures in implant-supported rehabilitation (8).

Changes in morphological aspects and chemical composition of implant surfaces affect the dynamics of bone healing at bone-implant contact area during the initial stages after implant placement (9). Several studies demonstrated that rough titanium surfaces induce the activation of platelets to release growth factors (10), improves osteogenesis (11), affects the degree of osseointegration (12), and enhances mechanical stability (13). Additionally, surface energy affects the biological response to the implant, it is believed that hydrophilic surfaces tend to enhance the early stages of cell adhesion, proliferation, differentiation, and bone mineralization compared to hydrophobic surfaces (14). Thus, wettability probably controls the proteins capable of adsord to the surface and the formation of a blood clot and a fibrin network (15). It is believed that the interaction between roughness and surface hydrophilicity can create a favourable microenvironment to reduce healing times and increase osseointegration, however, it seems that increased wettability of the surface had a stronger immunomodulatory effect than increased roughness (16). Clinical studies showed 5-year cumulative success rate above 96% (17,18) and a robust bone-implant contact (BIC), ranging from 67 to 81% on implants treated by grit-blasting and etching (19). Recent methods deal with electrochemical procedures for biomimetic functionalization of dental implants. Functionalization by using bioactive ceramics aims to mimic the natural deposition of calcium phosphate apatite crystals on the implant surfaces leading to the precipitation of biological apatite on the surface of the implant (20,21).

Electrical stimulation of the bone after implant placement has been studied in the last years (22,23). An invasive electrochemical method, and most commonly used, is the direct current (DC) stimulus, approved by the Food and Drug Administration (FDA) in 1979. DC stimulus consists of a battery that generates an electric field (EF) to growing cells, either directly through the implant device or indirectly through the medium where they are growing (24) and has been used clinically for over 36 years thenceforth for fracture healing (25). On the other hand, non-invasive approaches for bone growth stimulation namely inductive

stimulus has been reported in literature, which through external electrodes generates an EF, and capacitive stimulus, which from coils connected in series generates an electromagnetic field (24,26). In fact, electric stimulus speeds up bone formation process, probably stimulating the migration of pre-existing osteoblasts and mesenchymal cells to the implant-bone interface during the first stage of the osseointegration process. Several experimental *in vitro* and *in vivo* studies (22,23,27–30) and clinical success (31,32) are reported in literature. Furthermore, electrical stimulation is considered an adjunctive procedure for bone healing complication treatment, especially in high-risk patients (33). However, the underlying mechanism by which electrically induced osteogenesis occurs remains unclear, thus, additional research and high-quality study designs are needed to determine the most effective treatment modalities and pathologies best used with bone stimulation.

There is no consensus in the literature regarding the operating principles of both electric current densities $0.01\ A/m^2<J<0.5\ A/m^2$ (24) and amplitudes 7 μA to 50 μA (25) applied in the bone-dental implant interface. However, titanium implants submitted to 20 μA electrical current application for 14 days showed better bone apposition on the implant surface with 82% BIC and 44 μm on peripheral bone area ($p<0.01$). This result shows the positive correlation between the percentage of bone-implant contact and the application of electric current of 20 μA (23). To our knowledge, experimental studies have not involved different clinical situations linked to the implant design, electrical source site, and the bone conditions.

Considering several factors that affect the osseointegration process, finite element analyses can also be a good strategy to preliminary distinguish key aspects to enhance osseointegration of implants. In this way, it is possible to evaluate different parameters separately leading to a proper planning of *in vitro* and *in vivo* studies. The aim of this study was to evaluate the influence of different density and amplitude of electric current on the percentage of bone-implant contact using the finite element method. The null hypothesis of this study was that the ideal electrical current application is around 20 μA and that the position of the current source inside the implant influences the BIC area.

5.3 MATERIAL AND METHODS

5.3.1 Numerical model of the implant-battery-bone assembly

The numerical model used in the present study was designed from the histomorphometric evaluation of the bone implant contact after *in vivo* electrical stimulation of dental implants (23). Commercially pure titanium (cp Ti) grade IV implants were connected to a 1.5 V battery with an electrical resistance (*R*) at 150 kΩ on 10 µA or at 75 kΩ on 20 µA. The average current density for 10 µA at body/apex peri-implant region is 66 mA/m^2, and at cervical region is 175 mA/m^2 and for 20 µA at body/apex peri-implant region is 132 mA/m^2 and at cervical region is 350 mA/ m^2. The distance (*h*) of the electrical current source and the electrical current flow (*I*) are shown in Figure 1. The geometric details on the implant and battery can also be seen in Figure 1. The dielectric properties of the materials involved in the implant-battery-bone set up are described in Table 1.

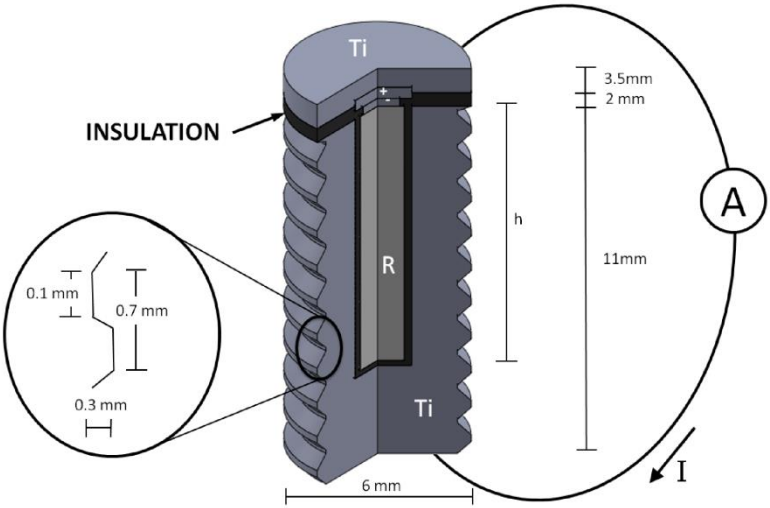

Figure 1. Schematic illustration of the implant-battery geometry. Cross-sectioned drawing reveals internal design of the implant connected to the battery. Distance (*h*); electrical current flow (*I*); electrical resistance (*R*) and titanium dental implant (Ti).

Table 1 – Dielectric properties of materials and tissues involved in the study.

Description	Electric conductivity σ (S/m)	Relative permittivity ε_r	References
Cp Ti grade IV	2.5×10^{6}	1.6×10^{2}	(34,35)
Insulating (nylon)	1×10^{-12}	8	(36)
Cancellous bone	2×10^{-1}	1×10^{3}	(37)
Cortical bone	2×10^{-2}	5×10^{2}	(37,38)
Soft tissue	4×10^{-2}	6×10^{4}	(38)

Details of the implant to bone interface are shown in Figure 2A. The representative section of the implant-bone region was selected according to previous studies considering a cancellous bone with 21 mm in height (37), cortical bone with 1 mm in height (37,38) soft tissue with 2 mm in thickness (38), and blood clot with 0.3-0.6 mm in thickness (39). The equivalent electric circuit related to the implant-battery and peri-implant tissues is shown in Figure 2B, where R_{Ti} is the electrical resistance for cp Ti while R_{TiO2} is the electrical resistance for TiO_2 and blood clot (BC); R_B is the electrical resistance for the cancellous and cortical bone and R_S is the electrical resistance for soft tissue. The total electrical current flowing on the dental implant and surrounding tissues is represented by I_T (Fig. 2B).

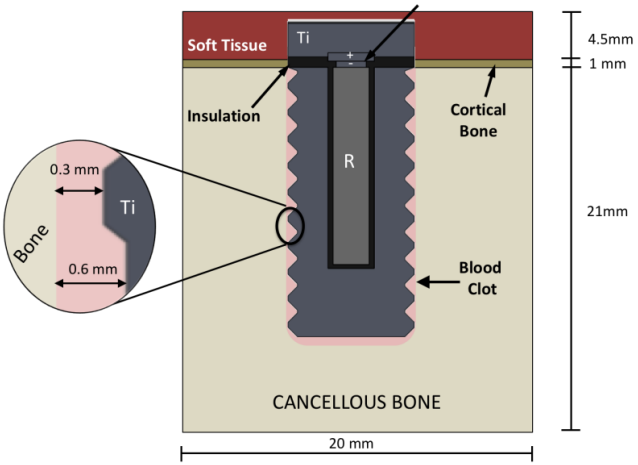

(A)

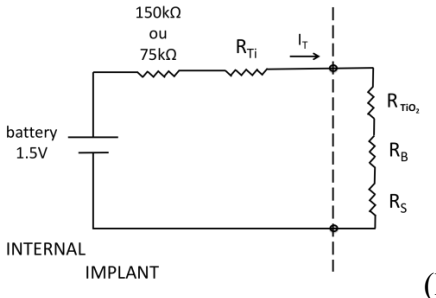

(B)

Figure 2. Schematics of the implant and batter surrounded by the peri-implant tissues. (A) The implant to bone region is shown in details according to previous studies (39), being: electrical resistance (*R*) and titanium dental implant (Ti). (B) Equivalent electric circuit of the dental implant and surrounding tissues, where total electrical current flowing on the dental implant and surrounding tissues (I_T); titanium electrical resistance (R_{Ti}); TiO_2 and blood clot (BC) resistance (R_{TiO2}); cancellous and cortical bone resistance (R_B) and soft tissue resistance (R_S).

5.3.2 Finite element analysis

Three-dimensional (3D) model calculations were run on a personal computer (Intel Core i5-2500, 3.3 GHz, 4 GB RAM) with Windows 7 (x64; Microsoft, Inc., Redmond, WA, USA) operating system. The electric field distribution on the implant-battery assembly and peri-implant tissues was computed by finite element method (FEM) using the COMSOL Multiphysics® (Stockholm, Sweden). A grid independence study was performed to establish an optimized mesh. This numerical model generated 96,185 tetrahedral elements by FEM. The local electric field (*E*) value at each one of the tetrahedral elements calculating dominion was determined by a steady current module (AC/DC module) following the Laplace equation as follow:

$$-\nabla \cdot (\sigma \nabla \cdot V) = 0 \qquad (1)$$

where σ is the tissue conductivity (S/m) that is dependent on the electric field and *V* is the electric potential. Neumann's boundary condition was applied for external insulate surfaces while interface between different materials were assessed by Dirichlet's boundary condition (36).

5.3.3 Parameters models

Current computational limitations do not allow simulating dimensions of titanium oxide thickness (nanometres) and implant dimensions (millimetres) simultaneously. To work around this dimensional difference of more than 100,000 times, the oxide and clot were considered to be a single macroscopic system with specific electrical characteristics. These electrical characteristics were obtained through the compatibilization of the electrical conductivity of this medium with the experimental results obtained by Bins-Ely (23). The electrical conductivity ($\sigma_{BC+TiO2}$) of the implant to bone region was simulated from 0.05 to 0.5 S/m. The relative permittivity was considered similar to that recorded for blood ($4x10^3$ (40)). The experimental and simulated bone-implant region (23) were compared to those of dental implants with resistance at 150 kΩ and 75 kΩ. The electrical current was applied at about 10 μA for 150 kΩ or 20 μA for 75 kΩ.

The percentage of simulated bone-implant region was analysed within an electric current ranging from 1 up to 60 μA and $\sigma_{BC+TiO2}$= 0.30 S/m. The variation of electric current application was simulated for cervical (h=5 mm) and apical peri-implant region (h=10 mm). The ideal current density for osseointegration 0.01 A/m^2<J<0.5 A/m^2 was illustrated by colours. A low current density for osseointegration (J<0.01 A/ m^2) was represented in black colour while high current density (J> 0.5 A/m^2) was suggested in white colour (24).

5.4 RESULTS

The initial evaluation of the electric current source on the implant simulation revealed an electrical current intensity at 10.5 μA for 150 kΩ and 21.1 μA for 75 kΩ.

Electrical conductivity of the implant-bone gap region filled by blood clot was below 0.45 S/m on an electric current source at 20 μA.

In the simulation, $\sigma_{BC+TiO2}$ variation was between 0.05 and 0.5 S/m and it was verified that for the current source of 20 μA all these values would be acceptable. Therefore, they would not give evidence of which electrical conductivity value should be chosen for the model. The limiting value was the $\sigma_{BC+TiO2}$ for 10 μA current source. Electrical conductivity ($\sigma_{BC+TiO2}$) for 0.05 to 0.2 S/m presented BIC (%) values obtained experimentally for 10 μA as shown by Figure 3. Figure 3 also

shows that 0.35 S / m is the threshold value from which the experimental results show a smaller area of osseointegration.

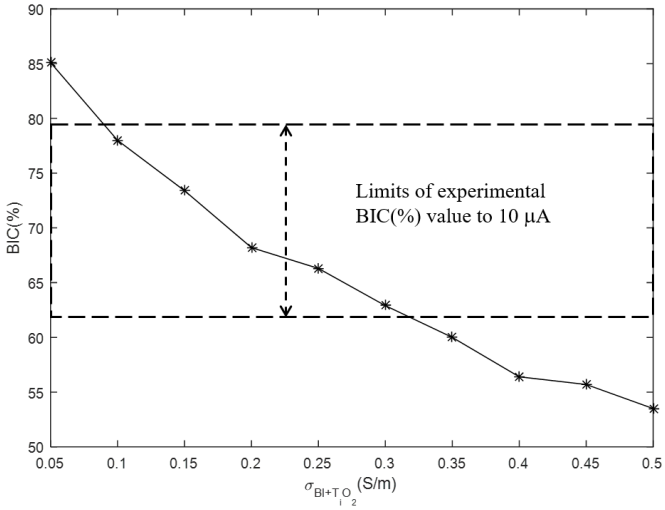

Figure 3. Electrical conductivity of the blood clot region. The arrow delimits the experimental variations of BIC (%) results to 10 µA obtained by (23).

The current density distribution (J) though the implant on $\sigma_{BC+TiO2}$ = 0.3 S/m is shown in Figure 4. This high conductivity value generates a low resistance value, which brings the worst hypothesis for the study, underestimating the osseointegration area. The total electric current applied to the implant (A) and (C) was at 10 µA, (B) and (D) was 20 µA.

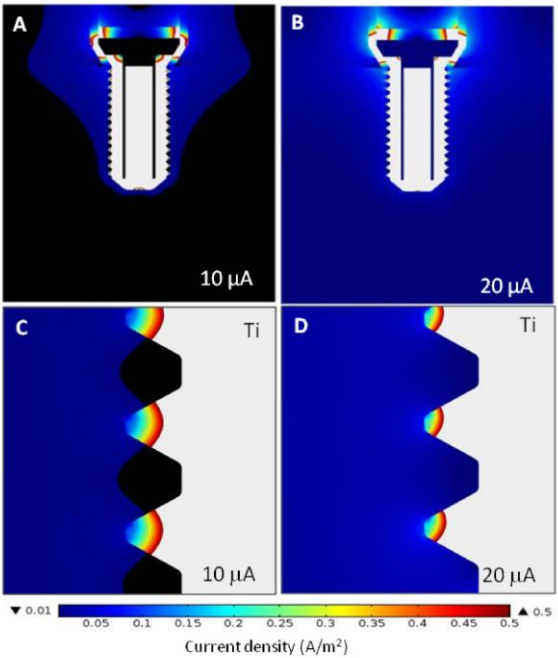

Figure 4. Distribution of current density on implant for (A,C) 10 µA and (B,D) 20 µA. $\sigma_{BC+TiO2}$=0.3 S/m. (C,D) The bone-implant interface shown in details. Black colour indicated J<0.01 A/m^2 while rainbow colour was at 0.01 A/m^2<J<0.5 A/m^2, and white at J> 0.5 A/m^2,

The implications of electrical current source on the bone-implant contact percentage are shown in Figures 5 and 6. Electrical conductivity ($\sigma_{BC+TiO2}$) was 0.3 S/m for both graphics. However, in Figure 5, electrical current application was performed at the apical peri-implant region (h = 10 mm) and showed a BIC of 80% for application of 20 µA; 93% for application of 30 µA and 98% for application of 40 µA. On the other hand, in Figure 6, electrical current application was performed at cervical peri-implant region (h = 5 mm) and showed lower BIC (%) for all current source applied.

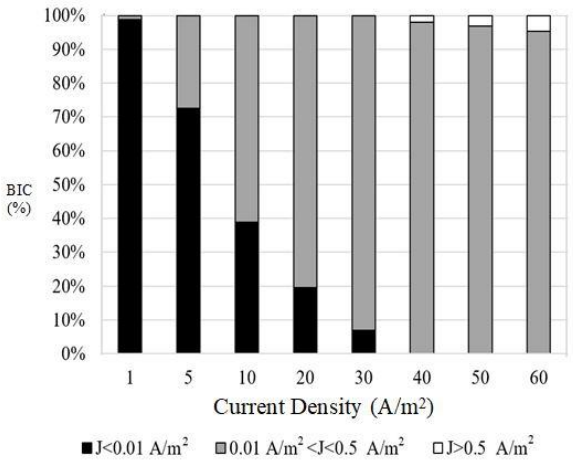

Figure 5. Influence of the current source variation on the bone-implant contact (BIC) percentage. $\sigma_{BC+TiO2}$=0.3 S/m. h = 10 mm, current applied at the apical peri-implant region.

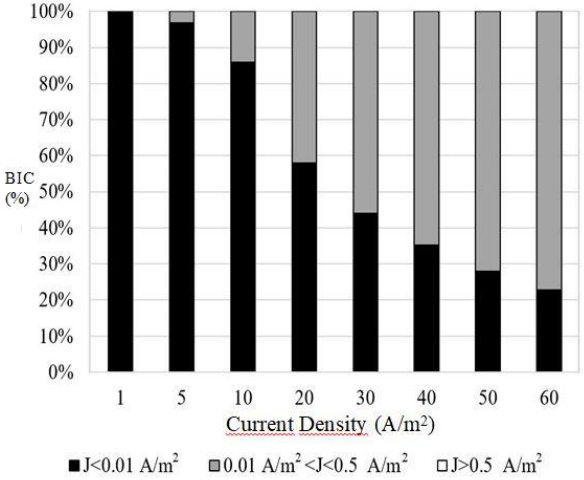

Figure 6. Influence of the current source variation on the bone-implant contact (BIC) percentage. $\sigma_{BC+TiO2}$=0.3 S/m. h = 5 mm, current applied in the cervical peri-implant region.

5.5 DISCUSSION

The results of the present study support the rejection of the null hypothesis. They showed that a source applying a direct and constant electric current below 10 μA does not evidenced acceptable current density for osseointegration (BIC < 55%). However, current sources of 10 to 20 μA and 30 to 40 μA presented BIC above 60% and 90%, respectively. In relation to implant geometry, the application of the current source at the apical peri-implant region, closer to the implant apex, resulted in 86.1% of the BIC area.

The electrical conductivity of the titanium oxide formed in the dental implant is approximately 10^{-6} S/m (41) and thickness of 1-10 nm (42,43) blood has 0.6 S/m (44,45) and mean thickness of 0.45 mm (39). Considering the surface area of the implant in contact with the oxide equal to that of the oxide and the clot covering the implant, an equivalent conductivity closer to the blood can be estimated. The value obtained in this work was 0.3 S/m (Fig. 3). However, the blood between the implant and the bone undergoes a coagulation process. The blood conductivity decreases during coagulation. This reduction in conductivity may be approximately 10 times the value between coagulated and uncoagulated sample (46). This process of coagulation (and consequently, its conductivity) depends on several factors such as temperature, blood sedimentation and hematocrit (47). It is difficult to estimate its value at the time of the experiment. Thus, the value obtained in this study is compatible with the expected value for the analytical approach. Using only blood (0.6 S/m (40)) at the implant-bone interface in the simulations did not present similar results obtained experimentally. The interface titanium and blood clot still have a thin layer of titanium oxide (~ 20nm). However, both the oxide thickness and the TiO_2 conductivity (between 10^{-7} (48) and 10^{6} S/m (34)) were difficult to estimate. Therefore, to evaluate the electrical and geometric properties of TiO_2 and blood clot independent in the experimental conditions was a limitation of this study. The conductivity of the clot with TiO_2 in the medium, at the implant-bone interface, was considered adequate between 0.10 and 0.30 S/m, values lower than blood conductivity. Thus, the numerical model simulation evaluated the TiO_2 and the clot together, presenting macroscopically a constant electrical conductivity ($\sigma_{BC+TiO2}$). However, several studies have shown that the electrical conductivity of titanium oxide depends on the applied electric field (35,49). In this study, it was considered that the electric field is not

enough to produce alteration in the conduction mechanisms of TiO_2. In the model, the coagulation process is already established and its electrical conductivity does not change (50,51).

An issue that remains unclear is regarding an optimal dosage of electrical stimulation, related to both density and intensity of applied electric current, especially considering the variation in bone density in different individuals. Experimental studies have not followed any standardized technique, making it difficult to compare studies or to draw conclusions for suitable application to human situations. Common parameters applied include fixed DC currents of 1-50 μA/cm^2 which can affect osteoblast proliferation and expression of differentiation markers (24,27,52). Published literature reports different direct current amplitudes, ranging from 7 to 50 μA, to induce bone formation (25), while bone formation has been enhanced in tibiae and femurs of rabbits or dogs after electrical stimulation at 10–20 μA over different periods of time (53). Figure 4 shows the current density distribution (J) though the implant on $\sigma_{BC+TiO2}$ = 0.3 S/m, whereas qualitatively high conductivity value generates a low resistance value, underestimating the osseointegration area. Especially at the top of the thread, bone-implant interface presents slightly better results (rainbow color), while in the valley region, the density is equal to or less than 0.15 A/m^2, demonstrating that the macrogeometry could alter the current density distribution at different regions of the implant.

Based on literature, Bins-Ely et al. (23) showed that the increase in BIC area was higher when electrical stimuli were applied, as evidenced by statistically significant differences between the tests (10 μA and 20 μA) and control (0 μA) groups after 15 d ($p < 0.01$). However, the numerical model demonstrated better results for BIC area when applied electric current of 30 and 40 μA (90%) and BIC area of 60% for current sources of 10 and 20 μA (Fig. 5), divergent from classical literature, that showed that thirty microamperes or more causes osteonecrosis (54).

Narkhede (55) demonstrated in his study, in rabbit, that a weak stimulus (20 μA) did not show much difference from the control group. And prolonged periods of electrical stimulation with 100 μA were detrimental to the process of bone formation. Gittens et al. (24) suggests that an applied electric current of more than 40 μA exhibit an electrical current density greater than 0.5 A/m^2, which may cause tissue damage. Corroborating with this finding, another study reported electrochemically reduction in oxygen tension and a considerable elevation in pH occurred at 100 μA, known to cause necrosis in vivo

(53). At the soft tissue level, direct current can promote vascular permeability, angiogenesis (56), and formation of new skin (57). It is believed that the desirable effect of tissue healing occurs with the application of electric current between 20 and 40 μA (57,58).

In despite of the current flow is not uniform along the surrounding bone–implant interface (23), previous studies have also reported bone formation after electrical stimulation associated with dental implants placed in dog mandible (28,59). Therefore, questioned whether the implant design, more specifically, the position of the electric current source inside the prototype - cervical vs. apical peri-implant regions, could change the BIC area rates. This mathematical model showed that the application of the ideal current source of 20 μA is at the bottom of the implant, apical peri-implant region (h=10 mm), resulting in 86.1% of the BIC area (Fig. 5). While in the applications at the cervical peri-implant region results in a reduction around 10% of the area (Fig. 6). However, although 75.4% of the BIC area has acceptable current density for osseointegration, its distribution is heterogeneous, presenting $I<0.01$ A/m^2 at the apical peri-implant region. Yet, it can be concluded that due to the high conductivity of Ti, the application of the source in different regions of the implant does not cause significant changes in BIC area (%).

The simulation was carried out statically over time. Thus, the implant deterioration, possible physical-chemical reactions of the osseointegration process, due to oxidation (24). The implant was simulated alone, with no other implants or adjacent teeth likely to interfere with the passage of electrical current. This would increase the resistance (R) of Figure 2B. The changes in the value of current sources occur because in the implant this form of generation is dependent on the materials between the poles of the battery as shown in Figure 2 B. This change becomes important in the case of $\sigma_{BC+TiO2} \leq 0.1$ S/m, $I_T \leq 17.12$ μA. In this case, there is a reduction of more than 18% of the original 21 μA. However, this reduction is not sufficient to affect osseointegration (Figure 3). This mathematical model considered the healing cap submerged to the soft tissue (Figure 2A). Such information is relevant since that the healing cap exposed may changes the conductivity of the system. Such variables are being studied and will be described in a future article.

5.6 CONCLUSIONS

Within the limitations of a mathematical model of a previous *in vivo* study, the main outcomes of this work can be summarized as follows:

- Electrical current source applying below 10 μA might not provide a required resultant current density for osseointegration as indicated by bone-implant contact below 55%. However, electrical current sources ranging from 10 up to 20 μA could increase the bone-implant contact to about 60% while source ranging from 30 up to 40 μA can result in bone-implant contact at around 90%;
- Regarding the positioning of the electrical source, the application of the electrical current source at the apical peri-implant region, closer to the implant apex, resulted in 86.1% bone-implant contact. The electrical current source at the coronal region might decrease the bone-implant percentage;
- It is believed that the macrogeometry of the implant thread may play a role on the current density at the bone-implant interface. This, and the fact that healing caps exposed may change the electrical conductivity of the system, are subjects that will be discussed in a future article.
- New approaches associated with electrical stimulation will contribute to the advancement of modern conventional dental implant technology and will be applied to various situations related to bone formation. Thus, by accelerating the osseointegration, the treatment time will be shortened, especially in patients with low quality and insufficient bone quantity and high-risk patients.

5.7 REFERENCES

1. Brånemark PI, Hansson BO, Adell R, Breine U, Lindström J, Hallén O OA. Osseointegrated implants in the treatment of the edentulous jaw. Experience from a 10-year period. Scand J Plast Reconstr Surg Suppl. 1977;16:1–132.

2. Esposito M, Ardebeli Y, Worthington H V. Interventions for replacing missing teeth: different types of dental implants. Cochrane Database Syst Rev. 2014;(7).

3. van Velzen FJJ, Ofec R, Schulten EAJM, ten Bruggenkate CM. 10-year survival rate and the incidence of peri-implant disease of 374 titanium dental implants with a SLA surface: A prospective cohort study in 177 fully and partially edentulous patients. Clin Oral Implants Res. 2015;26:1121–8.

4. Albrektsson T, Wennerberg A. Oral implant surfaces: Part 2 - review focusing on clinical knowledge of different surfaces. Int J Prosthodont. 2004;17(5):544–64.

5. de Groot RJ, Oomens MAEM, Forouzanfar T, Schulten EAJM. Bone augmentation followed by implant surgery in the edentulous mandible: A systematic review. J Oral Rehabil. 2018;45:334–43.

6. Schiegnitz E, Al-Nawas B. Bilal Al-Nawas, Prof Dr Dr Augmentation procedures using bone substitute materials or autogenous bone-a systematic review and meta-analysis.

7. Chrcanovic B, Albrektsson T, Wennerberg A. Bone Quality and Quantity and Dental Implant Failure: A Systematic Review and Meta-analysis. Int J Prosthodont [Internet]. 2017;30(3):219–37. Available from: http://quintpub.com/journals/ijp/abstract.php?iss2_id=1446&article_id=17160&article=3&title=Bone Quality and Quantity and Dental Implant Failure: A Systematic Review and Meta-analysis#.WQNgP_1JmG8

8. Esposito M, Grusovin MG, Maghaireh H WH. Interventions for replacing missing teeth: different times for loading dental implants (Review). Cochrane Database Syst Rev. 2013;(3):6–96.

9. Koshy E, Philip SR. Dental Implant Surfaces: An Overview. Int J Clin Implant Dent. 2015;1(1):14–22.

10. Himmlova L, Kubies D, Hulejova H, Bartova J, Riedel T, Stikarova J, et al. Effect of Blood Component Coatings of Enosseal Implants on Proliferation and Synthetic Activity of Human Osteoblasts and Cytokine Production of Peripheral Blood Mononuclear Cells. Mediators Inflamm. 2016;1–15.

11. Davies J. Understanding peri-implant endosseous healing. J Dent Educ. 2003;67(8):932–49.

12. Salou L, Hoornaert A, Louarn G, Layrolle P. Enhanced osseointegration of titanium implants with nanostructured surfaces: An experimental study in rabbits. Acta Biomater. 2015;494–502.

13. Bosshardt DD, Chappuis V, Buser D. Osseointegration of titanium, titanium alloy and zirconia dental implants: current knowledge and open questions. Periodontology 2000. 2017.

14. Gittens RA, Scheideler L, Rupp F, Hyzy SL, Geis-Gerstorfer J, Schwartz Z, et al. A review on the wettability of dental implant surfaces II: Biological and clinical aspects. Acta Biomaterialia. 2014.

15. Kopf BS, Ruch S, Berner S, Spencer ND, Maniura-Weber K. The role of nanostructures and hydrophilicity in osseointegration: In-vitro protein-adsorption and blood-interaction studies. J Biomed Mater Res - Part A. 2015;

16. Hotchkiss KM, Reddy GB, Hyzy SL, Schwartz Z, Boyan BD, Olivares-Navarrete R. Titanium surface characteristics, including topography and wettability, alter macrophage activation. Acta Biomater. 2016;31:425–34.

17. Lethaus B, Kalber J, Petrin G, Brandstatter A, Weingart D. Early Loading of Sandblasted and Acid-Etched Titanium Implants in the Edentulous Mandible. Int J Oral Maxillofac Implant. 2011;26:887–92.

18. Cochran D, Jackson J, Bernard J, Bruggenkate CM ten, Buser D, Taylos T, et al. 5 Year Prospective Multicenter Study of Early Loaded Titanium Implants with a Sandblasted and Acid-Etched Surface. Int J Oral Maxillofac Implant. 2011;26:1324–32.

19. Nevins M, Parma-Benfenati S, Quinti F, Galletti P, Sava C, Sava C, et al. Clinical and Histologic Evaluations of SLA Dental Implants. Int J Periodontics Restorative Dent. 2017;

20. Le Guéhennec L, Soueidan A, Layrolle P, Amouriq Y. Surface treatments of titanium dental implants for rapid osseointegration. Dent Mater. 2007;23(7):844–54.

21. Ribeiro AR, Oliveira F, Boldrini LC, Leite PE, Falagan-Lotsch P, Linhares ABR, et al. Micro-arc oxidation as a tool to develop multifunctional calcium-rich surfaces for dental implant applications. Mater Sci Eng C. 2015;54:196–206.

22. Song JK, Cho TH, Pan H, Song YM, Kim IS, Lee TH, et al. An electronic device for accelerating bone formation in tissues surrounding a dental implant. Bioelectromagnetics. 2009;30:374–84.

23. Bins-Ely LM, Cordero EB, Souza JCM, Teughels W, Benfatti CAM, Magini RS. In vivo electrical application on titanium implants stimulating bone formation. J Periodontal Res. 2017;52(3).

24. Gittens RA, Olivares-Navarrete R, Tannenbaum R, Boyan BD, Schwartz Z. Electrical Implications of Corrosion for Osseointegration of Titanium Implants. J Dent Res [Internet]. 2011;90(12):1389–97. Available from: http://journals.sagepub.com/doi/10.1177/0022034511408428

25. Nelson FRT, Brighton CT, Ryaby J, Simon BJ, Nielson JH, Lorich DG, et al. Use of physical forces in bone healing. J Am Acad Orthop Surg. 2003;11:344–54.

26. Cochran BVG. Experimental methods for stimulation of bone healing by means of electrical energy. Bull N Y Acad Med. 1972;48(7):899–911.

27. Kim IS, Song JK, Zhang YL, Lee TH, Cho TH, Song YM, et al. Biphasic electric current stimulates proliferation and induces VEGF production in osteoblasts. Biochim Biophys Acta - Mol Cell Res. 2006;

28. Shayesteh YS, Eslami B, Dehghan MM, Vaziri H, Alikhassi M, Mangoli A, et al. The effect of a constant electrical field on osseointegration after immediate implantation in dog mandibles: A preliminary study: Basic science research. J Prosthodont. 2007;16(5):337–42.

29. Wang J, Tang N, Xiao Q, Zhang L, Li Y, Li J, et al. Pulsed electromagnetic field may accelerate in vitro endochondral ossification. Bioelectromagnetics. 2015;36:35–44.

30. Barak S, Neuman M, Iezzi G, Piattelli A, Perrotti V, Gabet Y. A new device for improving dental implants anchorage: A histological and micro-computed tomography study in the rabbit. Clinical Oral Implants Research. 2015;

31. Brighton C, Friedenberg Z, Mitchell E, Booth R. Brighton,1977. Treatment of nonunion with constant direct current. Clin Orthop Relat Res. 1977;124:106–23.

32. Kleczynski S. Electrical stimulation to promote the union of fractures. Int Orthop. 1988;12:83–7.

33. Cook JJ, Summers NJ, Cook EA. Healing in the New Millennium: Bone Stimulators: An Overview of Where We've Been and Where We May be Heading. Clin Podiatr Med Surg. 2015;32(1):45–59.

34. Donachie MJ. Titanium: a technical guide. ASM international; 2000.

35. Diebold U. The surface science of titanium dioxide. Surf Sci Rep. 2003;48:53–229.

36. Sadiku MNO. Elements of Electromagnetics. 6th ed. Oxford University Press, editor. 2014.

37. Li T, Hu K, Cheng L, Ding Y, Ding Y, Shao J, et al. Optimum selection of the dental implant diameter and length in the posterior mandible with poor bone quality - A 3D finite element analysis. Appl Math Model. 2011;35:446–456.

38. Kim HJ, Yun HS, Park H Do, Kim DH, Park YC. Soft-tissue and cortical-bone thickness at orthodontic implant sites. Am J Orthod Dentofac Orthop. 2006;130:177–82.

39. Vanegas-Acosta JC, Landinez P. NS, Garzón-Alvarado DA. Mathematical model of the coagulation in the bone-dental implant interface. Comput Biol Med. 2010;40:791–801.

40. Gabriel S, Lau RW, Gabriel C. The dielectric properties of biological tissues: III. Parametric models for the dielectric spectrum of tissues. Phys Med Biol. IOP Publishing; 1996;41(11):2271.

41. Pan J, Thierry D, Leygraf C. Hydrogen peroxide toward enhanced oxide growth on titanium in PBS solution: Blue coloration and clinical relevance. J Biomed Mater Res Vol 30, 393-402. 1996;30:393–402.

42. Guo CY, Matinlinna JP, Tang ATH. Effects of surface charges on dental implants: Past, present, and future. Int J Biomater. 2012;2012:1–5.

43. Gittens RA, Olivares-Navarrete R, Rettew R, Butera RJ, Alamgir FM, Boyan BD, et al. Electrical polarization of titanium surfaces for the enhancement of osteoblast differentiation. Bioelectromagnetics. 2013;34:599–612.

44. Peratta C, Peratta A. Modelling the human body expouse to ELF electric fields. Wessex Institute of Technology Press, editor. UK; 2010. 160 p.

45. Gabriel C, Gabriel S, Corthout E. The dielectric properties of biological tissues: I. Literature survey. Phys Med Biol [Internet]. 1996;41:2231–49. Available from: http://iopscience.iop.org/0031-9155/41/11/001

46. Ur A. Detection of Clot Retraction Through Changes of the Electrical Impedance of Blood during Coagulation. Am J Clin Pathol [Internet]. 1971;56:713–8. Available from: http://ajcp.oxfordjournals.org/

47. Ramaswamy B, Yeh YTT, Zheng SY. Microfluidic device and system for point-of-care blood coagulation measurement based on electrical impedance sensing. Sensors Actuators, B Chem. 2013;180:21–7.

48. Regonini D, Adamaki V, Bowen CR, Pennock SR, Taylor J, Dent ACE. AC electrical properties of TiO 2 and Magnéli phases, Ti n O 2n − 1. Solid State Ionics [Internet]. 2012;229:38–44. Available from: http://dx.doi.org/10.1016/j.ssi.2012.10.003

49. Jankowski B. Preparation and electrical properties of Ti-TiO2-Metal thin film structures. Thin Solid Films. 1976;34:69–72.

50. Lei KF, Chen KH, Tsui PH, Tsang NM. Real-Time Electrical Impedimetric Monitoring of Blood Coagulation Process under Temperature and Hematocrit Variations Conducted in a Microfluidic Chip. PLoS One. 2013;8(10):e76243.

51. Hayashi Y, Brun MA, Machida K, Nagasawa M. Principles of Dielectric Blood Coagulometry as a Comprehensive Coagulation Test. Anal Chem. 2015;87:10072−10079.

52. Bodamyali T, Kanczler J, Simon B, Blake D, Stevens C. Effect of Faradic Products on Direct Current-Stimulated Calvarial Organ Culture Calcium Levels. Biochem Biophys Res Commun. 1999;264:657–61.

53. Brighton C, Friedenberg Z, Zemsky LM, Pollis P. Direct-current stimulation of non-union and congenital pseudarthrosis. Exploration of its clinica application. l. J Bone Jt Surg. 1975;57(3):368–77.

54. Friedenberg Z, Zemsky L, Pollis R. The Response of Non-Traumatized Bone to Direct Current. JBJS. 1974;56(5):1023–30.

55. Narkhede PR. A histologic evaluantion of the effect of electrical stimulation on osteogenic changes following placement of blade-vent implants in the mandible of rabbits. J Oral Implantol. 1998;24(4):185–95.

56. Poltawski L, Watson T. Bioelectricity and microcurrent therapy for tissue healing – a narrative review. Phys Ther Rev. 2009;14(2):104–14.

57. Chu C-S, McManus A, Mason AJA, Okerberg C, Pruitt BJ. Multiple graft harvestingd from deep partial-thickness scald wound healed under the incluence of weak Direct Current. J Trauma. 1990;30(8):1044–9.

58. Kloth LC. Electrical Stimulation for Wound Healing: A Review of Evidence From In Vitro Studies, Animal Experiments, and Clinical Trials. Int J Low Extrem Wounds. 2005;4(1):23–44.

59. Shigino, Ochi, Kagami, Sakaguchi, Nakade. Application of Capacitivel y Coupled Electric Field Enhances Periimplant Osteogenesis in the Dog Mandible. Int J Prosthodont. 2000;13(5):365–72.

6 METODOLOGIA EXPANDIDA

6.1 CONCEITOS BÁSICOS EM ELETROQUÍMICA

6.1.1 Piezoeletricidade e Lei de Wolff

O efeito piezoelétrico é uma resposta biológica ao estímulo mecânico, documentada por Fukada e Yasuda (FUKADA; YASUDA, 1957) ao observar no osso a produção de carga elétrica negativa em áreas de compressão e carga elétrica positiva nas áreas de tração. Esta propriedade causa a resposta celular que leva ao crescimento ósseo proposto pela lei de Wolff. Em termos simples, o osso é uma fonte de energia elétrica endógena quando é mecanicamente estressado ou lesionado, a tensão leva ao aumento da formação óssea e a pressão leva à reabsorção óssea (BEHARI, 1991). O uso de fontes de energia, como os danos elétricos, poderia, portanto, aumentar ou mesmo acelerar a formação óssea em torno dos implantes dentários, particularmente em áreas de baixa qualidade óssea (BRIGHTON et al., 1975).

No entanto, hoje sabe-se que o remodelamento ósseo está relacionado ao fenômeno da transdução mecânica, e não ao efeito piezoelétrico. Este é apenas um marcador do fluxo de fluido, que provoca ativação de canais iônicos mecanossensíveis, principalmente os canais de cálcio e potássio, alterando o potencial da membrana celular positiva (despolarização) ou negativamente (hiperpolarização). A hiperpolarização está associada à osteogênese, enquanto a despolarização, com reabsorção óssea (RIDDLE; DONAHUE, 2009). Por outro lado, a mecanotransdução pode ser resumida da seguinte forma: o estresse mecânico aplicado a um osso na escala macroscópica é transformado em um sinal que as células ósseas são capazes de detectar. A natureza e a magnitude deste sinal são pouco conhecidos (STROE; CROLET; RACILA, 2013).

6.1.2 Fundamentos de Circuitos Elétricos

Circuito Elétrico é uma interconexão de elementos elétricos.
Carga é uma propriedade elétrica das partículas atômicas que compõe a matéria, medida em coulombs (C). A matéria, por sua vez, é formada por elementos fundamentais chamados átomos, que são constituídos por elétrons (carga negativa), prótons (carga positiva) e nêutrons. E uma das

suas principais características é o fato de ser móvel (fluxo de cargas elétricas).

Quando um fio condutor (formado por átomos) é acoplado a uma bateria (uma fonte de força eletromotriz) as cargas são obrigadas a se mover. Cargas negativas se movem em uma direção, enquanto cargas positivas se movem na direção contrária, essa movimentação dá-se o nome de corrente elétrica. Portanto, corrente elétrica é o fluxo de carga por unidade de tempo, medido em ampères (A).

A intensidade da corrente é determinada pela quantidade de carga elétrica por unidade de tempo. Assim, temos:

$$i = \frac{dq}{dt}$$

Unidades no Sistema Internacional:
q = carga elétrica → coulomb (C);
Δt = intervalo de tempo → segundo (s);
i = intensidade de corrente elétrica → coulomb por segundo (C/s) = ampere (A).

Corrente contínua (CC) é uma corrente que permanece constante ao longo do tempo, conhecida pelo símbolo I.
Corrente alternada (CA) é uma corrente que varia com o tempo segundo uma forma de onda senoidal, conhecida pelo símbolo i.

Por outro lado, a densidade de corrente elétrica é o vetor de magnitude igual à quantidade de carga elétrica por unidade de tempo, em que a corrente elétrica constante passa em determinada área superficial. Assim, a densidade de corrente (J) é definida pela corrente elétrica (i), por unidade de área (A), medida em ampères (A) por metro quadrado (m^2):

J = i / A

Para deslocar o elétron em um condutor a determinado sentido é necessário algum trabalho ou transferência de energia. Esse trabalho é realizado por uma força eletromotriz externa, também conhecida como tensão ou diferença de potencial. A tensão V_{ab} entre dois pontos *a* e *b*

em um circuito elétrico é a energia (ou trabalho) necessária para deslocar uma carga unitária de *a* para *b*; matematicamente:

$$v = \frac{dw}{dq}$$

w = energia → joules (J)
q = carga elétrica → coulomb (C)
V = tensão → volts (V)
Assim: 1 volt = 1 joule/coulomb = 1 newton-metro/coulomb

Resistência elétrica é a propriedade física de um material de resistir à passagem de corrente elétrica, mesmo quando existe uma diferença de potencial aplicada. É representada pelo símbolo *R* e é medida em ohms (Ω).
A resistência de qualquer material com uma área da seção transversal (*A*) uniforme depende de *A* e de seu comprimento l.
A resistência de um condutor depende da resistividade do material. A resistividade, por sua vez, depende da temperatura na qual o condutor se encontra e independe da geometria da amostra. Assim temos:

$$R = \rho \frac{\ell}{A}$$

ρ é a resistividade elétrica do condutor (Ω.m)
R é a resistência elétrica do material (Ω)
l é o comprimento do condutor (m)
A é a área da seção do condutor (m^2)

A lei de Ohm relaciona a corrente I – ou taxa de passagem de cargas ao longo do tempo – à voltagem aplicada V da seguinte maneira:

V = I.R

Ou seja: para um condutor mantido à temperatura constate, a razão entre tensão (V) (entre dois pontos) e a corrente elétrica (I) é constante. Esta constante é a resistência elétrica (R). De acordo com a convenção de sinal passivo, a corrente flui de um potencial maior para um menor.

Outra medida importante para análise de circuitos é o inverso da resistência *R*, conhecida como condutância *(G)*, uma medida que representa quanto um elemento conduz corrente elétrica:

$$G = \frac{1}{R} = \frac{I}{V}$$

A unidade de condutância é o *mho* (ohm escrito ao contrário), com símbolo, o ômega invertido. Mas a unidade SI é o siemens (S):

$$1\,S = 1\,\mho = 1\,A/V$$

Portanto, Condutância é a capacidade de um elemento conduzir corrente elétrica, medida em siemens (S).

Condutividade elétrica (σ) é usada para especificar a natureza elétrica de um material. É o inverso da resistividade (ρ). Ou seja, é a indicativa da facilidade na qual um material é capaz de conduzir uma corrente elétrica.
A unidade é o inverso de ohm-metro, isto é, $[(\Omega\text{-m})^{-1}]$ ou mho/m (= S/m).

$$\sigma = \frac{1}{\rho}$$

Uma forma de classificar os materiais sólidos é de acordo com a facilidade com que conduzem a corrente elétrica: condutores, semicondutores e isolantes. Metais são bons condutores, tipicamente apresentando condutividade da ordem de 10^7 $(\Omega\text{-m})^{-1}$.

Um matérial dielétrico é um isolante elétrico, não metálico, no qual é possível produzir e manter um campo elétrico com pequeno ou nenhum suprimento de energia de fontes externas.

Capacitor: é um dispositivo constituído por dois condutores, cada um tendo uma determinada superfície exposta ao outro, separados por um meio isolante. Uma diferença de potencial entre os dois condutores acarreta em armazenamento de cargas iguais em intensidade e de polaridades opostas. Os dois condutores são chamados eletrodos.

Capacitância: é a propriedade de um capacitor ou de um sistema de condutores e dielétricos que permite armazenar cargas separadas eletricamente, quando existem diferenças de potencial entre os condutores.
Ou seja, quando uma voltagem é aplicada através de um capacitor, uma das placas torna-se positivamente carregada, e a outra negativamente, com o campo elétrico correspondente direcionado da positiva para negativa. Uma carga Q é acumulada em cada placa do capacitor e é diretamente proporcional à tensão aplicada e à área das placas e inversamente proporcional à distancia entre elas:

$$C = \frac{Q}{V}$$

Permissividade relativa (ε_r) ou constante dielétrica (k) do material compara a capacidade de um material, entre duas placas, em direcionar suas cargas na aplicação de uma voltagem, em relação ao vácuo. Indica quantas vezes a capacidade do sistema foi aumentada com a introdução deste material (isolante) entre as placas do capacitor.

A variação na capacitância C é o reflexo direto da constante dielétrica do material, onde Q é a carga armazenada (em Coulombs) e V é a voltagem através dos condutores (ou placas). A unidade é Coulombs por volt ou farad (F). A constante dielétrica é uma propriedade dos materiais de consideração fundamental para a construção de um capacitor.

Fonte: (ALEXANDER; SADIKU, 2013; CALLISTER JR, 2007)

6.2 SIMULAÇÃO NUMÉRICA

6.2.1 Aquisição dos dados e descrição do modelo

Os dados geométricos do modelo foram obtidos do estudo *in vivo* realizado em tíbia de cães por Bins-Ely et al. (BINS-ELY et al., 2017). Informações histológicas e características elétricas dos tecidos circundantes e dos materiais envolvidos foram encontrados na literatura. Os resultados histomorfométricos do contato osso-implante (BIC) após a estimulação elétrica *in vivo* de implantes dentários (BINS-ELY et al., 2017) e os achados literários foram usados como referência para construção dos cálculos numéricos.

Na sequência, essas informações foram incorporadas ao simulador. Implantes de titânio comercialmente puro grau IV (Ti cp) foram conectados a uma bateria de 1,5 V com uma resistência elétrica (R) a 150 kΩ em 10 μA ou a 75 kΩ em 20 μA. A densidade de corrente média para 10 μA na região peri-implantar corpo/ápice é 66 mA/m^2, e na região cervical é 175 mA/m^2 e para 20 μA na região peri-implantar corpo/ápice é 132 mA/m^2 e na região cervical é 350 mA/m^2. A distância (h) da fonte de corrente elétrica e o fluxo de corrente elétrica (I), assim como os detalhes geométricos do implante e da bateria podem ser vistos na Figura 1 (página 31). As propriedades dielétricas dos materiais envolvidos no desenho implante-osso-bateria são descritos na Tabela 1 (página 31).

Foram desenhados modelos que consideraram o corte do implante (titânio comercialmente puro grau IV) instalado em osso, cortical e medular, envolto por coágulo e protegido por tecido mole, na superfície, na forma de paralelepípedo. Depois, cada domínio foi caracterizado eletricamente conforme dados da literatura. Detalhes do implante na interface óssea são mostrados na Figura 2A (página 33).

A seção representativa da região implante-osso foi selecionada de acordo com estudos anteriores considerando um osso esponjoso com 21 mm de altura (LI et al., 2011), osso cortical com 1 mm de altura (KIM et al., 2006; LI et al., 2011) tecido mole com 2 mm de espessura (KIM et al., 2006; MOTOYOSHI et al., 2007) e coágulo de sangue com espessura de 0,3-0,6 mm (DIEBOLD, 2003). O circuito elétrico equivalente relacionado à bateria de implante e tecidos peri-implantares é mostrado na Figura 2B, onde R_{Ti} é a resistência elétrica para Ti cp enquanto R_{TiO2} é a resistência elétrica para TiO^2 e coágulo sanguíneo (BC); R_B é a resistência elétrica para o osso esponjoso e cortical e R_S é a resistência elétrica para tecido mole. A corrente elétrica total que flui no implante dentário e nos tecidos adjacentes é representada pela I_T (Fig. 2B) (página 33).

6.2.2 Modelagem numérica

Os cálculos do modelo tridimensional (3D) foram executados em um computador pessoal (Intel Core i5-2500, 3,3 GHz, 4 GB de RAM) com o sistema operacional Windows 7 (x64; Microsoft, Inc., Redmond, WA, EUA). A distribuição do campo elétrico no conjunto implante-bateria e nos tecidos peri-implantar foi calculada pelo método

dos elementos finitos (FEM) usando o COMSOL Multiphysics® (Estocolmo, Suécia).

As simulações realizadas são estacionárias, ou seja, supõe-se que o sistema está em regime permanente, não considerando o tempo como uma variável.

Elaborar a malha, ou domínio de calculo, é um processo crítico, pois há diferença na escala das grandezas envolvidas, desde a espessura do coágulo ao comprimento do implante. Isto produz regiões finas e outras espessas, que são automaticamente ajustadas, pelo programa, às menores grandezas, o que resulta num elevado número de elementos, muitas vezes impedindo a construção das malhas. Dessa forma, FEM requer a segmentação da estrutura em análise, ou seja, dividir o modelo geométrico em regiões, com relação às dimensões envolvidas, e gerar malhas com granularidades distintas. A divisão do solido em elementos infinitesimais permite que o calculo seja executado rapidamente considerando as condições locais e dos elementos fronteiriços.
Este modelo numérico gerou 96.185 elementos tetraédricos por FEM. O valor do campo elétrico local (E) em cada um dos elementos tetraédricos calculando o domínio foi determinado por um módulo de corrente constante (módulo AC/CC) seguindo a equação de Laplace como segue:

$$-\nabla \cdot (\sigma \nabla \cdot V) = 0 \qquad (1)$$

onde σ é a condutividade do tecido (S / m) que depende do campo elétrico e V é o potencial elétrico. A condição de contorno de Neumann foi aplicada para superfícies isolantes externas, enquanto a interface entre diferentes materiais foi avaliada pela condição de contorno de Dirichlet (SADIKU, 2014).

6.2.3 Parâmetros da simulação

As atuais limitações computacionais não permitem simular dimensões da espessura do óxido de titânio (nanômetros) e dimensões do implante (milímetros) simultaneamente. Para contornar essa diferença dimensional de mais de 100.000 vezes, o óxido e o coágulo foram considerados como um único sistema macroscópico com características elétricas específicas. Essas características elétricas foram obtidas através da compatibilização da condutividade elétrica deste meio com os resultados experimentais obtidos por Bins-Ely (BINS-ELY et al., 2017). A condutividade elétrica ($\sigma_{BC+TiO2}$) da interface osso-implante

foi simulada de 0,05 a 0,5 S/m. A permissividade relativa (ε_r) foi considerada similar àquela registrada para sangue ($4x10^3$ (VANEGAS-ACOSTA; LANDINEZ P.; GARZÓN-ALVARADO, 2010)). O experimento e simulação da interface osso-implante (BINS-ELY et al., 2017) foi comparada com implantes dentários com resistência a 150 kΩ e 75 kΩ. A corrente elétrica foi aplicada ao redor de 10 µA para 150 kΩ ou 20 µA para 75 kΩ.

A porcentagem da simulação da interface osso-implante foi analisada dentro de uma corrente elétrica variando de 1 a 60 µA e $\sigma_{BC+TiO2}$= 0,30 S/m. A variação da aplicação de corrente elétrica foi simulada para a região peri-implantar cervical (h = 5 mm) e apical (h = 10 mm). A densidade de corrente ideal para a osseointegração 0,01 A/m^2 < J < 0,5 A/m^2 foi ilustrada por cores. Uma baixa densidade de corrente para osseointegração (J < 0,01 A/m^2) foi representada na cor preta, enquanto alta densidade de corrente (J > 0,5 A/m^2) foi sugerida na cor branca (GITTENS et al., 2011).

7 REFERÊNCIAS

AARON, R. K. et al. Clinical biophysics: The promotion of skeletal repair by physical forces. **Annals New York Academy of Sciences**, v. 1068, p. 513–531, 2006.

ALBREKTSSON, T. et al. OSSEOINTEGRATED TITANIUM IMPLANTS. **Acta orthop. scand. 52, 155-170, 1981** , v. 52, p. 155–170, 1981.

ALEXANDER, C. K.; SADIKU, M. N. O. **Fundamentos de Circuitos Elétricos**. 5. ed. ed. Porto Alegre: AMGH, 2013.

ARO, H. et al. Electrostimulation of rat callus cells and human lymphocytes in vitro. **Journal of Orthopaedic Research**, v. 2, p. 23–31, 1984.

BAGGI, L. et al. The influence of implant diameter and length on stress distribution of osseointegrated implants related to crestal bone geometry: A three-dimensional finite element analysis. **Journal of Prosthetic Dentistry**, 2008.

BASSETT, C. A. L.; PAWLUK, R. J.; PILLA, A. A. Acceleration of fracture repair by electromagnetic fields. A surgically noninvasive method. **Annals of the New York Academy of Sciences**, p. 242–262, 1974.

BEHARI, J. Electrostimulation and bone healing. **Crit Rev Biomed Eng.**, v. 18, n. 4, p. 235–254, 1991.

BINS-ELY, L. M. et al. In vivo electrical application on titanium implants stimulating bone formation. **Journal of Periodontal Research**, v. 52, p. 479–484, 2017.

BORDJI, K. et al. Cytocompatibility of Ti-6Al-4V and Ti-5Al-2.5Fe alloys according to three surface treatments, using human fibroblasts and osteoblasts. **Biomaterials**, v. 17, p. 929–940, 1996.

BRÅNEMARK PI, HANSSON BO, ADELL R, BREINE U, LINDSTRÖM J, HALLÉN O, O. A. Osseointegrated implants in the treatment of the edentulous jaw. Experience from a 10-year period. **Scand J Plast Reconstr Surg Suppl.**, v. 16, p. 1–132, 1977.

BRIGHTON, C. et al. Direct-current stimulation of non-union and congenital pseudarthrosis. Exploration of its clinica application. l. **Journal of Bone & Joint Surgery**, v. 57, n. 3, p. 368–377, 1975.

BRIGHTON, C. et al. Brighton,1977. Treatment of nonunion with constant direct current. **Clinical Orthopaedics and related research**, v. 124, p. 106–123, 1977.

BROGGINI et al. Peri-implant Inflammation Defined by the Implant-Abutment Interface. **J Dent Res**, v. 85, n. 5, p. 473–478, 2006.

BUCH, F.; ALBREKTSSON, T.; HERBST, E. Direct current influence on bone formation in titanium implants. **Biomaterials**, v. 5, p. 341–346, 1984.

BUSER, D. et al. Influence of surface characteristics on bone integration of titanium implants. A histomorphometric study in miniature pigs. **Journal of Biomedical Materials Research**, v. 25, p. 889–902, 1991.

CALLISTER JR, W. D. **Ciência e Engenharia de Materiais. Uma Introdução**. Sétima edi ed. Rio de Janeiro: LTC - Livros Técnicos e Científicos. Editora S.A., 2007.

COCHRAN, B. V. G. Experimental methods for stimulation of bone healing by means of electrical energy. **Bull. N. Y. Acad. Med.**, v. 48, n. 7, p. 899–911, 1972.

COELHO, P. G. et al. Osseointegration: Hierarchical designing encompassing the macrometer, micrometer, and nanometer length scales. **Dental Materials**, v. 31, p. 37–52, 2015.

COOK, J. J.; SUMMERS, N. J.; COOK, E. A. Healing in the New Millennium: Bone Stimulators: An Overview of Where We've Been and Where We May be Heading. **Clinics in Podiatric Medicine and Surgery**, v. 32, n. 1, p. 45–59, 2015.

CRUZ, H. V et al. Tribocorrosion and Bio-Tribocorrosion in the Oral Environment : The Case of of Dental Implants. In: J. PAULO DAVIM, P. (Ed.). . **Biomedical Tribology**. [s.l.] Nova Science Publishers, Inc., 2011. DIEBOLD, U. The surface science of titanium dioxide. **Surface science reports**, v. 48, n. 5, p. 53–229, 2003.

DUAN, K.; WANG, R. Surface modifications of bone implants through wet chemistry. **Journal of Materials Chemistry**, v. 16, p. 2309–2321, 2006.

ELIAS, C. N. et al. Relationship between surface properties (roughness, wettability and morphology) of titanium and dental implant removal torque. **Journal of the Mechanical Behavior of Biomedical Materials**, p. 234–242, 2008.

FRIEDENBERG, Z. B. et al. The Effects of Demineralized Bone Matrix and Direct Current on an "In Vivo" Culture of Bone Marrow Cells. **Journal of Orthopaedic Research**, v. 7, p. 22–27, 1989.

FUKADA; YASUDA. On the Piezoelectric Effect of Bone. **Journal of the physical society of japan**, v. 12, n. 10, p. 1158–1162, 1957.

GITTENS, R. A. et al. Electrical Implications of Corrosion for Osseointegration of Titanium Implants. **Journal of Dental Research**, v. 90, n. 12, p. 1389–1397, 2011.

HOTCHKISS, K. M. et al. Titanium surface characteristics, including topography and wettability, alter macrophage activation. **Acta Biomaterialia**, v. 31, p. 425–434, 2016.

HU, X. N.; YANG, B. C. Conformation change of bovine serum albumin induced by bioactive titanium metals and its effects on cell behaviors. **Journal of Biomedical Materials Research - Part A**, v. 102, n. 4, p. 1053–1062, 2014.

KILPADI, D. V; LEMONS, J. E. Surface characterization of unalloyed titanium implants. **Journal of Biomedical Materials Research**, v. 28, p. 1419–1425, 1994.

KIM, H. J. et al. Soft-tissue and cortical-bone thickness at orthodontic implant sites. **American Journal of Orthodontics and Dentofacial Orthopedics**, v. 130, p. 177–182, 2006.

KLECZYNSKI, S. Electrical stimulation to promote the union of fractures. **International Orthopaedics**, v. 12, p. 83–87, 1988.

KOPF, B. S. et al. The role of nanostructures and hydrophilicity in osseointegration: In-vitro protein-adsorption and blood-interaction studies. **Journal of Biomedical Materials Research - Part A**, 2015.

LAZZARA, R. J. Dental implant system design and its potential impact on the establishment and sustainability of aesthetics. **Journal of implant and reconstructive dentistry Edit.**, v. 19, p. 117–129, 2012.

LI, T. et al. Optimum selection of the dental implant diameter and length in the posterior mandible with poor bone quality - A 3D finite element analysis. **Applied Mathematical Modelling**, v. 35, p. 446–456, 2011.

LIMA, E. M. C. X. et al. Evaluation of surface characteristics of Ti-6Al-4V and Tilite alloys used for implant abutments. **Braz Oral Res**, v. 20, n. 4, p. 307–11, 2006.

LIU, X.; CHU, P. K.; DING, C. Surface modification of titanium, titanium alloys, and related materials for biomedical applications. **Materials Science and Engineering R: Reports**, v. 47, p. 49–121, 2004.

MOTOYOSHI, M. et al. Effect of Cortical Bone Thickness and Implant Placement Torque on Stability of Orthodontic Mini-implants. **INT J ORAL MAXILLOFAC IMPLANTS** , v. 22, p. 779–784, 2007.

NELSON, F. R. T. et al. Use of physical forces in bone healing. **The Journal of the American Academy of Orthopaedic Surgeons**, v. 11, p. 344–354, 2003.

PONSONNET, L. et al. Relationship between surface properties (roughness, wettability) of titanium and titanium alloys and cell behaviour. **Materials Science and Engineering C**, v. 23, p. 551–560, 2003.

QUIRYNEN, M.; DE SOETE, M.; VAN STEENBERGHE, D. Infectious risks for oral implants: A review of the literature. **Clinical Oral Implants Research**, v. 13, p. 1–19, 2002.

RIDDLE, R. C.; DONAHUE, H. J. From Streaming potentials to shear stress: 25 years of bone cel mechanotransduction. **J Orthop Res**, v. 27, p. 143–149, 2009.

ROOS-JANSAKER et al. Nine- to fourteen-year follow-up of implant treatment. Part III: Factors associated with peri-implant lesions. **Journal of Clinical Periodontology**, v. 33, p. 296–301, 2006.

SADIKU, M. N. O. **Elements of Electromagnetics**. 6. ed. [s.l: s.n.].
SELA, M. N. et al. Adsorption of human plasma proteins to modified titanium surfaces. **Clinical Oral Implants Research**, v. 18, p. 630–638, 2007.

SEZIN; CROHARÉ; IBANEZ. Microscopic Study of Surface Microtopographic Characteristics of Dental Implants. **The Open Dentistry Journal**, v. 10, p. 139–147, 2016.

SHAFER, D. M. et al. The Effect of Electrical Perturbation on Osseointegration of Titanium Dental Implants: A Preliminary Study. **J Oral Maxillofac Surg**, v. 53, p. 1063–1068, 1995.

SHAYESTEH, Y. S. et al. The effect of a constant electrical field on osseointegration after immediate implantation in dog mandibles: A preliminary study: Basic science research. **Journal of Prosthodontics**, v. 16, n. 5, p. 337–342, 2007.

SHIGINO, T. et al. Enhancing Osseointegration by Capacitively Coupled Electric Field: A Pilot Study on Early Occlusal Loading in the Dog Mandible. **Int J Oral Maxillofac Implants**, v. 16, p. 841–850, 2001.

SONG, J. K. et al. An electronic device for accelerating bone formation in tissues surrounding a dental implant. **Bioelectromagnetics**, v. 30, p. 374–384, 2009.

STEINEMANN, S. G. Titanium - The material of choice? **Periodontology 2000**, v. 17, p. 7–21, 1998.

STROE, M. C.; CROLET, J. M.; RACILA, M. Mechanotransduction in cortical bone and the role of piezoelectricity: A numerical approach. **Computer Methods in Biomechanics and Biomedical Engineering**, v. 16, n. 2, p. 119–129, 2013.

TEUGHELS, W. et al. Effect of material characteristics and/or surface topography on biofilm development. **Clin. Oral Imp. Res**, v. 17, p. 68–81, 2006.

THOMAS, K. A.; COOK, S. D. An evaluation of variables influencing implant fixation by direct bone apposition. v. 19, p. 875–901, 1985.

VANEGAS-ACOSTA, J. C.; LANDINEZ P., N. S.; GARZÓN-ALVARADO, D. A. Mathematical model of the coagulation in the bone-dental implant interface. **Computers in Biology and Medicine**, v. 40, p. 791–801, 2010.

VERDONK, R. et al. Biological methods to enhance bone healing and fracture repair. **Arthroscopy - Journal of Arthroscopic and Related Surgery**, v. 31, n. 4, p. 715–718, 2015.

VERVAEKE; COLLAERT; DE BRUYN. The effect of implant surface modifications on survival and bone loss of immediately loaded implants in the edentulous mandible. **Int J Oral Maxillofac Implants**, v. 28, p. 1352–1357, 2013.

WEBER, H.-P. et al. Proceedings of the Fourth ITI Con-sensus Conference, sponsored by the International Team for Implan-tology (ITI) and held. **The International Journal of Oral & Maxillofacial Implants**, v. 24, p. 180–183, 2009.

8 APÊNDICE

Journal of
PERIODONTAL RESEARCH

J Periodont Res 2017; 52: 479–484

JOURNAL OF PERIODONTAL RESEARCH
doi:10.1111/jre.12413

In vivo electrical application on titanium implants stimulating bone formation

L. M. Bins-Ely[1], E. B. Cordero[1], J. C. M. Souza[1], W. Teughels[2], C. A. M. Benfatti[1], R. S. Magini[1]
[1]Center for Research on Dental Implants (CEPID), School of Dentistry (ODT), Universidade Federal de Santa Catarina (UFSC), Florianópolis, Santa Catarina, Brazil and [2]Department of Oral Health Sciences and University Hospitals Leuven, Katholieke Universiteit Leuven, Leuven, Belgium

Bins-Ely LM, Cordero EB, Souza JCM, Teughels W, Benfatti CAM, Magini RS. In vivo electrical application on titanium implants stimulating bone formation. J Periodont Res 2017; 52: 479–484. © 2016 John Wiley & Sons A/S. Published by John Wiley & Sons Ltd

Background and Objective: The aim of the present *in vivo* study was to measure the bone implant contact area after electrical stimulation of dental implants.

Material and Methods: Ninety titanium dental implants (6 mm × 11.5 mm) with a smooth surface were placed in six male Beagle dogs and then the implant-bone interfaces was assessed by histological analyses after 7 and 15 d. The 12-mo-old dogs, with a weight of 15 kg, were randomly divided into two groups based on the duration of bone healing: 7 and 15 d. Also, implants were divided into three groups based on electrical stimulation: group A, 10 μA; group B, 20 μA; and group C, control group. The electrical current was applied by an electrical device coupled to the implant connection.

Results: After 7 d of electrical stimulation, no statistical differences in bone–implant interface contact area were observed. However, a significantly higher bone–implant interface contact area was recorded for group B than for groups A and C ($p < 0.01$) after 15 d. No statistical difference was observed between groups A and C ($p > 0.05$).

Conclusion: The electrical stimulation of dental implants can generate a larger area of bone–implant interface contact as a result of bone formation. Factors such as different electrical current intensity and duration should be studied in further work to clarify the potential of this method.

Ricardo de Souza Magini, DDS, MSc, PhD, Center for Research on Dental Implants (CEPID), School of Dentistry (ODT), Universidade Federal de Santa Catarina (UFSC), Campus Trindade, Florianópolis, Santa Catarina 88040-900, Brazil
Tel: +55 48 37219077
Fax: 37219077
e-mails: ricardo.magini@gmail.com; cesarbenfatti@yahoo.com

Key words: bone formation; electrical stimulation; titanium implant

Accepted for publication July 22, 2016

Osseointegration is defined as the structural and functional direct contact between healthy bone and the implant surface without interference from connective tissue (1). There are two different phenomena by which bone can become deposited on the implant surface: (i) distance osteogenesis, in which new bone reaches the surface of the implant by appositional growth of existing peri-implant bone; and (ii) contact osteogenesis or osteoconduction, which relies on the recruitment and migration of osteogenic cells to the implant surface and *de novo* bone formation. Although all bone-healing sites will display both osteogenesis phenomena, the biological significance of these different healing reactions is extremely important, both to improve the role of implant design in endosseous integration and in elucidating the differences in the structure and composition of the bone–implant interface (2). The biocompatibility, design and surface characteristics of the implant, the host condition, the surgical technique and the load magnitude after implant placement influence the process of osseointegration and are important to achieve a long term success (3). The time required to accomplish the osseointegration process depends on the amount of bone–implant contact (BIC) and also on its mechanical and physiologic integrity against incident forces or inflammatory reactions (2,4). Traditionally, an osseointegration period of approximately 6 mo in the maxilla and 3 mo in the mandible was respected (5). Novel implant surfaces have been developed in order to accelerate bone formation and consequently to shorten the time before functional loading of the implant (6).

Different surface treatments have been performed in order to modify the titanium topography at a micro- and nano-scale, such as: grit-blasting followed by acid etching (7); plasma spraying (8); anodizing; calcium phosphate depositioning; or combinations of these techniques (9). Such surface modifications can enhance osteogenesis, resulting in an acceleration of the bone-formation process (6,10,11). Also, implant surface modification can increase the surface energy and wettability, leading to a higher adsorption of proteins and cells on the surface. This results in an improvement of the bone apposition rate (2). Several studies have been performed to explain the influence of the titanium surface energy on cellular behavior (12). The most widely accepted theory is that surface energy has a selective effect on the configuration and conformation of proteins that are adsorbed on the substrate (13 15).

An alternative to biochemical osteoinductive therapies is biophysical treatment, such as mechanical, electrical and sonic stimulation (16). There are three electrical stimulation methods commonly used for bone tissue-engineering applications, namely direct current and capacitive or inductive coupling methods. Direct current has been the method most commonly applied for fracture treatment in refractory or deficient bone healing (17). Previous studies (18) have shown that electrical signals, similar to those generated by bone stress mechanisms, may improve fracture healing. The main hypothesis is that the application of an electrical potential regulates cell signaling in bone formation, which significantly influences the bone repair process (19,20).

In *in vitro* studies, an electrical field can be applied across the surface on which the cells are growing, or indirectly through the culture medium (21), in order to evaluate bone growth phenomena. Different currents can be applied. A current ranging from 1 μA to 50 μA can stimulate the proliferation of osteoblasts (22) as well as the expression of growth factors for bone differentiation (23).

The main aim of this *in vivo* study was to assess the effect of electrical stimulation (direct current) on the bone-implant interface contact area around dental implants placed in dogs.

Material and methods

The experimental protocol of the present study was approved by the The Animal Ethics and Research Committee of Health Sciences at the Federal University of Santa Catarina, Florianópolis/SC, Brazil (concept # 114/CEUA/PRPe/2008). All items of the Animal Research: Reporting of In Vivo Experiments (ARRIVE) guidelines for animal research were followed in this study. One hour before the surgical procedure, six 12-mo-old male Beagle dogs, with a weight of 15 kg received an intramuscular injection of 0.44 mg/kg atropine sulfate (Atropinon®; Hipolabor Farmacêutica Ltda., Sabará, MG, Brazil). After 10 min, 3 mg/kg xylazine was administered (Rompun®; Bayer S. A., São Paulo, SP, Brazil), together with 16 mg/kg ketamine (Francotar®; Virbac, Saúde Animal, São Paulo, SP, Brazil), both by the intramuscular route, as a single dose. The Beagle dogs were divided randomly into two groups of either 7 or 15 d bone-healing periods (three dogs per evaluation period). A longitudinal incision on the tibia of each animal (Fig. 1A) was performed, in order to expose the underlying osseous tissue (Fig. 1).

Thirty-six titanium dental implants (6 mm in diameter and 11.5 mm in length), with machined surfaces (Lousan Usinagem Industrial, Joinville, Brazil), were placed 2 mm below the crestal bone of the tibia (Fig. 1B) after osteotomy by using a series of graded diameter drills to achieve the proper implant diameter. The osteotomy was carried out under constant irrigation with saline solution at room temperature. The implants were divided into three groups based on the intensity of electrical stimulation: group A, 10 μA; group B, 20 μA; and group C, control group. Each dog received five implants in their tibia in a randomized distribution concerning the electrical current source. The electrical current was applied by an electronic device coupled to the implant connection area, as shown in Figures 1C and 2.

The implants and the electronic devices were applied according to the groups. The surgical wound edges were sutured (Fig. 1D) in two planes, using 5.0 absorbable Vicryl thread (Ethicon-Vicryl®; Johnson & Johnson, São Paulo, SP, Brazil) and 4.0 nylon thread (Somerville®; Jaboatão dos Guararapes, Pernambuco, Brazil). During the evaluation period, the dogs were individually housed in ventilated barren cages, according to the ARRIVE guidelines for animal research. Then, the dogs were induced to a painless death, by administration of a lethal dose of sodium thiopental (Thionembutal®, São Bernardo do Campo, Sao Paulo, Brazil), 7 or 15 d after implant placement.

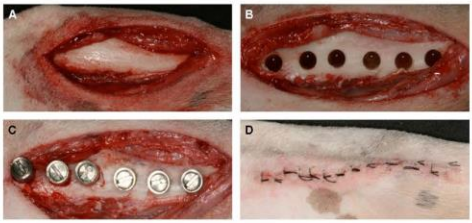

Fig. 1. Implants placed into the tibia of a Beagle dog. (A) Surgical incision exposing the tibia, (B) implants placed in bone, (C) electronic devices coupled to the implants, and (D) suturing of the wound edges.

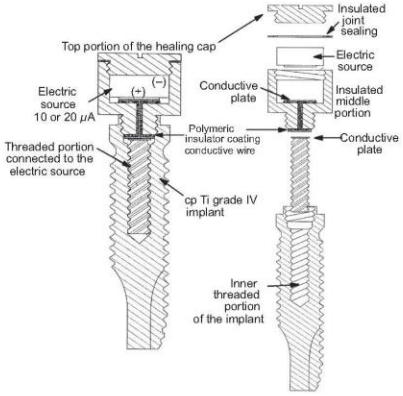

Fig. 2. Schematics of the implant and electronic device. cp Ti, commercially pure titanium.

Histology

The samples were kept in 10% formalin solution for 24 h after harvesting and were washed in distilled water. Then, samples were dehydrated through a series of graded ethanol baths (50%, 70%, 80%, 90% and 100%). After dehydration, the samples were embedded in methacrylate-based resins (Technovit 7200; Heraeus Kulzer GmbH, Wehrheim Germany), according to the manufacturer's recommendations. Samples of 50 μm thickness were obtained by cross-sectioning along the length axis of the implant at its medial zone using a precision cutting machine (Exact Apparatebau GmbH & Co., Norderstedt, Germany). Finally, samples were stained by applying Toluidine blue (Merck KGaA, Darmstadt, Germany) and acidic fuchsin (Merck). Optical microscopy was carried out at ×50 and ×100 magnifications using an optical microscope (Leica IC50 HD; Leica Microsystems, Heerbrugg, Switzerland) coupled to a computer. The analysis and measurement of the BIC area were performed by a researcher, blinded and well-trained on histomorphometry, using AxioVision software (Carl Zeiss, Hamburg, Germany).

Statistical analysis

The results were statistically analyzed using one-way ANOVA at a significance level of 5% ($p < 0.05$). Kruskal Wallis nonparametric tests were applied when required. Tukey's test was used for multiple comparisons.

Results

The mean values of the BIC area are shown in Tables 1 and 2.

The histomorphometry results showed no evidence of a BIC area after 7 d of electrical stimulation (Fig. 3). After 7 d, histomorphometric analyses showed the presence of a provisional matrix (which occurs before bone formation) surrounding the implants (Fig. 3). That provisional matrix was composed of blood clot and organized fibrin network. However, new-bone formation was detected around the implant after electrical stimulation for 15 d (Table 1). After 15 d of electrical stimulation, a significantly higher percentage of bone implant interface contact area was recorded in group B (20 μA of electrical stimulation) when compared with group A (10 μA of electrical stimulation) and group C (no stimulation) (82.3 ± 16.0% vs. 70.1 ± 9.6% vs. 51.0 ± 7.1%, respectively; $p < 0.01$) (Table 1 and Fig. 4). Also, the peripheral bone-formation area induced by distance osteogenesis increased in groups receiving electrical stimulation (groups A and B), as seen in Table 2. No statistical difference was noted between groups A and C ($p > 0.05$), as shown in Tables 1 and 2. No inflammatory cell infiltrate, foreign body reaction cells or multinucleated giant cells were found in the implant groups.

Discussion

In this study, the bone implant interface contact area was measured after application of different intensities of direct electric current. The increase in BIC area was higher when electrical stimuli were applied, as evidenced by statistically significant differences between the test (20 μA) and control (0 μA) groups after 15 d ($p < 0.01$). Also, the bone growth induced by distance osteogenesis increased in test groups receiving electrical stimulation (Table 2).

In the present study, the histomorphometry results showed no evidence of increased BIC area after 7 d of electrical stimulation. In fact, the electrical current flow is not uniform along the surrounding implant area

Table 1. Bone–implant contact (BIC) over a period of 15 d

Group	Electrical stimulation (μA)	BIC length (μm)	BIC (%)
A	10	510.45 ± 68.69	70.1 ± 9.6
B	20	591.20 ± 122.00	82.3 ± 16.0
C (control)	0	366.46 ± 51.26	51.0 ± 7.1

Values are given as mean ± SD. The groups with electrical stimulation (groups A and B) showed a significant increase in bone–implant contact area ($p < 0.01$).

Table 2. Measurements on peripheral bone area

Group	Electrical stimulation (μA)	Value (μm)
A	10[a]	24.269,70 ± 10.953,08
B	20[b]	44.751,68 ± 15.304,34
C (control)	0[a]	18.490.84 ± 7.139,48

Values are given as mean ± SD.
[a]Lower contact of the bone area, and [b]higher contact of the bone area, when comparing the areas of group A (10 μA) and group C (control), which showed no statistical difference ($p > 0.05$).

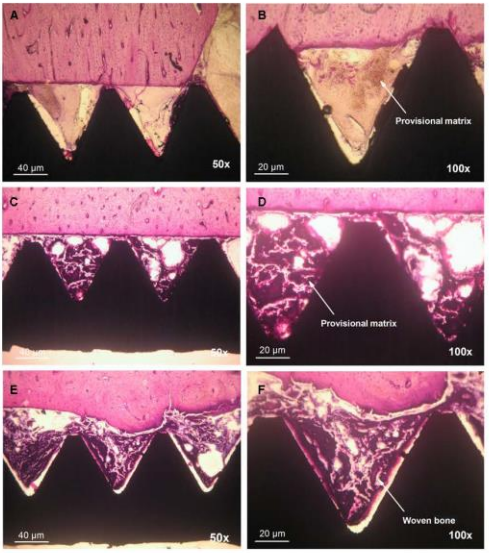

Fig. 3. Micrographs obtained by optical microscopy at ×50 and ×100 magnifications. Peri-implant area without (control group) (A, B) and after (C, D) stimulation with 10 μA electrical current for 7 d: blood clot and organized fibrin network can be observed. (E, F) Peri-implant area revealing immature bone as well as the beginning of bone formation after stimulation with 20 μA electrical current for 7 d.

because of the presence of a provisional matrix composed of a blood clot and fibrin network proteins and then subsequently because of bone tissue formation. The electrical current flow is established by following the path of least resistance between the implant and the surrounding environment. Consequently, some areas can have a high current density, whereas others can have low current density. This current path stimulates the growth of bone tissue in the vicinity of the implant (20,23,24). In fact, bone formation can be mainly affected by the current flow path for 7 d of electrical stimulation. Nevertheless, a significantly higher contact area of the bone implant interface was recorded after 20 μA (group B) of electrical stimulation for 15 d compared with 10 μA (group A) and 0 μA (group C) of electrical stimulation for the same time period ($p < 0.01$). Even though the current flow is not uniform along the surrounding bone implant interface, previous studies have also reported bone formation after electrical stimulation associated with dental implants placed in dog mandible (24–27). Electrical stimulation at 20 μA has also been shown to stimulate bone formation around dental implants in the jaw of dogs (27). After 30 d of direct electrical current application, the results showed a significant increase in BIC area compared with the control group. Another study reported the effect of a biphasic electrical current stimulator attached to a titanium implant, applying a current density of 20 μA/cm^2, on bone formation. After 7 d, that biphasic electrical current device was removed and replaced by conventional temporary healing abutment. The results revealed a higher BIC area after 15 and 30 d of healing (28). On the other hand, other studies evaluated the effect of 7 or 7.5 μA of electrical stimulation on dental implants placed in the mandible of rabbits (29,30). The authors reported that the application of 7 or 7.5 μA of electrical stimulation did not promote bone growth around dental implants (30).

Published literature reports different direct current amplitudes, ranging from 7 to 50 μA, to induce bone formation (16). However, bone necrosis has been reported when a high electrical current is used, while bone formation has been enhanced in tibiae and femurs of rabbits or dogs after electrical stimulation at 10 20 μA over different periods of time (31,32). In that direct electrical circuit, the titanium implant is a cathode, while bone and the surrounding tissues is the anode that allows the flow of electrical current (22). Around the cathode, reactions take place which reduce the oxygen concentration, resulting in the

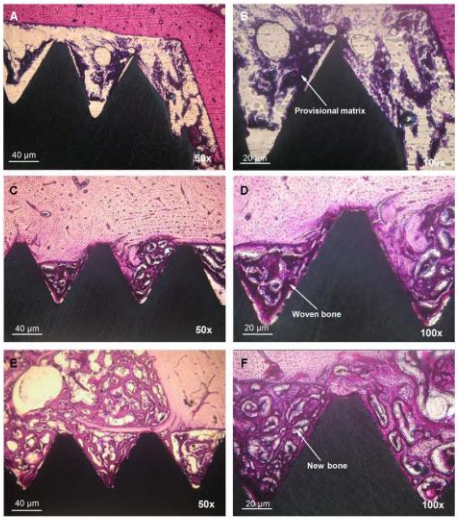

Fig. 4. Micrographs obtained by optical microscopy at ×50 and ×100 magnifications. (A, B) Peri-implant area free of current stimulation revealing blood clot and organized fibrin network. (C, D) Peri-implant area revealing immature bone after stimulation with 10 µA electrical current for 7 d. (E, F) Peri-implant area revealing higher contacting bone formation after stimulation with 20 µA of electrical current for 15 d.

production of hydroxyl radicals that increase the pH, according to the following equation (21,33,34):

$$O_2 + 2H_2O + 4e^- \rightarrow 4OH^- \quad \text{eqn 1}$$

The electrochemical reactions occurring at the cathode contribute to a constant electrical stimulation mechanism (33). The low oxygen concentration and alkaline environment at the surrounding tissues stimulate osteoblastic activity decreasing osteoclast activity. Additionally, hydrogen peroxide stimulates macrophages to release vascular endothelial growth factor (VEGF), which is an important angiogenic factor for bone healing (35). It is believed that continuous electrical stimulation regulates osteoinductive growth factors, such as bone morphogenetic proteins II, VI and VII, which are known as stimulators of cellular proliferation, differentiation and extracellular matrix synthesis of the bone and cartilage formation (27,36). This can increase bone formation induced by contact and distance osteogenesis, leading to a decrease in bone-healing time.

The selection of the test periods in our study was based on the bone-healing process around machined implants induced by distance osteogenesis in dogs (37). In distance osteogenesis, new bone is formed on the surfaces of old bone in the peri-implant site (2). The bone surfaces provide a population of osteogenic cells that lay down on a new matrix reaching the implant surface (2). Bone remodeling begins with an acceleration phase that lasts for hours or days, followed by bone resorption performed by osteoclasts. This period takes place in dogs for 10 d and in humans for 14 d. Then, the latency phase starts and lasts for 7 d in dogs and for approximately 7 14 d in humans. During that period osteoclasts are replaced by osteoblasts and bone formation begins. The osteoid matrix reaches the implant surface in dogs on the fourth week and in humans on the sixth week. Thus, the acceleration phase (7 d) corresponds to intense cell activity and capillary migration into the clot (angiogenesis) in humans. This explains why there was no statistical difference between the groups concerning histological analyses performed in this study. However, a higher inflammatory infiltrate was found in the control group. In humans, the resorption and latency phases for 15 d result in the merging of individual osteoid regions, leading to the process of bone-implant integration. The BIC area can indicate the degree to which that last process has been accomplished.

Conclusion

Within the limitations of this in vivo study, the main outcome of this work can be summarised as follows: bone-implant contact area significantly increased after electrical current stimulation at 20 µA applied on dental implants for 15 d.

Acknowledgements

The authors acknowledge the Brazilian financial support provided by CAPES and CNPq.

Conflict of interest statement

No conflict of interest.

Authors contributions

Letícia M. Bins-Ely: Data collection, Drafting article, Ernesto B. Cordero: Data collection, Data analysis/interpretation, Júlio C. M. Souza and Wim Teughels:Critical revision of article, Júlio C. M. Souza and Cesar A. M. Benfatti: Data analysis/

interpretation, Statistics, Ricardo S. Magini: Concept/Design, Approval of article, Funding secured.

References

1. Albrektsson TA. Multicenter report on osseointegrated oral implants. *J Prosthet Dent* 1988;**60**:75 84.
2. Davies JE. Understanding Peri-Implant Endosseus Healing 2005. *J Dent Educ.* 2003;**67**:932 949.
3. Albrektsson T, Brånemark PI, Hansson HA, Lindström J. Osseointegrated titanium implants. Requirements for ensuring a long-lasting, direct bone-to-implant Anchorage in man. *Acta Orthop Scand* 1981;**52**:155 170.
4. Jaffin RA, Berman CL. The excessive loss of Branemark fixtures in type IV bone: a 5-year analysis. *J Periodontol* 1991;**62**:2.
5. Puleo DA, Nanci A. Understanding and controlling the bone- implant interface. *Biomaterials* 1999;**20**:2311 2321.
6. Buser D, Schenk Rk, Steinemann S, Fiorellini Jp, Fox Ch, Stich H. Influence of surface characteristics on bone integration of titanium implants a histomorphometric study in miniature pig. *J Biomed Mater Res* 1991;**25**:889 902.
7. Orsini G, Assenza B, Scarana A, Piatelli M, Piatelli A. Surface analysis of machined versus sandblasted and acid-etched titanium implants. *Int J Oral Maxillofac Implants* 2000;**15**:779 784.
8. Ellingsen JE. Surface configurations of dental implants. *Periodontol 2000* 1998;**17**:36 46.
9. Yamagami A, Yoshihara Y, Suwa F. Mechanical and histologic examination of titanium alloy material treated by sandblasting and anodic oxidization. *Int J Oral Maxillofac Implants* 2005;**20**:48 53.
10. Gottlander M, Johansson CB, Wennerberg A, Albrektsson T, Radin S, Ducheyne P. Bone tissue reactions to an electrophoretically applied calcium phosphate coating. *Biomaterials* 1997;**18**:551 557.
11. Davies JE. Bone bonding at natural and biomaterial surface. *Biomaterials* 2007;**28**:5058 5067.
12. Kilpadi DV, Weimer JJ, Lemons JE. Effect of passivation and dry heat sterilization on surface energy and topography of unalloyed titanium implants. *Colloids Surf A Physicochem Eng Asp* 1998;**135**:89 101.
13. Baier RE, Meyer AE. Implant surface preparation. *Int J Oral Maxillofac Implants* 1988;**3**:9 20.
14. Uitto VJ, Larjava H, Peltonen J, Brunette DM. Expression of fibronectin and integrins in cultured periodontal ligament epithelial cells. *J Dent Res* 1992;**71**:1203 1211.
15. Aaron R, Ciombor D, Wang S, Simon B. Clinical biophysics: the promotion of skeletal repair by physical forces. *Ann N Y Acad Sci* 2006;**1068**:513 531.
16. Nelson FRT, Brighton CT, Ryaby J *et al.* Use of physical forces in bone healing. *J Am Acad Orthop Surg* 2003;**11**:344 354.
17. Ercan B, Webster TJ. The effect of biphasic electrical stimulation on osteoblast function at anodized nanotubular titanium surfaces. *Biomaterials* 2010;**31**: 3684 3693.
18. Yasuda I. Fundamental aspects of fracture treatment. *J Kyoto Med Soc* 1953;**4**: 395 406.
19. Bassett CAL, Becker RO. Generation of electric potentials by bone in response to mechanical stress. *Science* 1962;**137**:1063 1064.
20. Black J, Baranowski TJ, Brighton CT. Electrochemical aspects of DC stimulation of osteogenesis. *Bioelectroch Bioener* 1984;**12**:323 327.
21. Brighton CT, Black J, Friedenberg ZB, Esterhai JL, Day LJ, Connolly JF. A multicenter study of the treatment of nonunion with constant direct current. *J Bone Joint Surg Am* 1981;**63**:2 13.
22. Gittens RA, Olivares-Navarrete R, Tannenbaum R, Boyan BD, Schwartz Z. Electrical implications of corrosion for osseointegration of titanium implants. *J Den Res* 2011;**90**:1389 1397.
23. Kim IS, Song JK, Zhang YL, Lee TH, Cho TH, Song YM. Biphasic electric current stimulates proliferation and induces VEGF production in osteoblast. *Biochim Biophys Acta* 2006;**1763**:907 916.
24. Shigino T, Ochi M, Hirose Y, Hirayama H, Sakaguchi K. Enhancing osseointegration by capacitively coupled electric field: a pilot study on early occlusal loading in the dog mandible. *Int J Oral Maxillofac Implants* 2001;**16**:841 850.
25. Shigino T, Ochio M, Sakaguchi H, SaKaguchi K, Nakade O. Application of capacitevely coupled electric field enhances periimplant osteogenesis in the dog mandibule. *Int J Prosthodontic* 2000;**13**:365 372.
26. Shayesteh YS, Eslami B, Dehghan MM *et al.* The effect of a constant electrical field on osseointegration after immediate implantation in dog mandibles: a preliminary study. *J Prosthodont* 2007;**16**:337 342.
27. Gan JC, Fredericks DC, Glazer PA. Direct current and capacitive coupling electrical stimulation upregu- lates osteopromotive factors for spinal fusions. *Orthop J Harv Med Sch* 2004;**6**:57 59.
28. Song JK, Cho TH, Pan H *et al.* An electronic device for accelerating bone formation in tissues surrounding a dental implant. *Bioelectromagnetics* 2009;**30**: 374 384.
29. Shafer DM, Rogerson K, Norton L, Benneth J. The effect of electrical perturbation on osseointegration of titanium dental implants: a preliminary study. *J Oral Maxillofac Sur* 1995;**53**:1063 1068.
30. Dergin G, Aktas M, Gürsoy B, Kürkçü M, Devecioglu Y, Benliday E. Direct Current Electric Stimulation in Implant Osseointegration: an experimental animal study with sheep. *J Oral Implantol* 2013;**39**:671 679.
31. Friedenberg ZB, Andrews ET, Smolenski BI, Pearl BW, Brighton CT. Bone reaction to varying amounts of direct current. *Surg Gynecol Obstet* 1970;**131**: 894 899.
32. Brighton CT, Friedenberg ZB, Zemsky LZ, Pollis RP. Direct- current stimulation of non-union and congenital pseudoarthrosis. *J Bone Joint Surg* 1975;**57**: 368 377.
33. Bodamyali T, Kanczler JM, Simon B, Blake DR, Stevens CR. Effect of faradic products on direct current- stimulated calvarial organ culture calcium levels. *Biochem Biophys Res Commun* 1999;**264**: 657 661.
34. Bushinsky DA. Metabolic alka-losis decreases bone calcium efflux by suppressing osteoclasts and stimulating osteoblasts. *Am J Physiol* 1996;**271**:216 222.
35. Cho M, Hunt TK, Hussain MZ. Hydrogen peroxide stimulates macrophage vascular endothelial growth factor release. *Am J Physiol Heart Circ Physiol* 2001;**280**:2357 2363.
36. Fredericks DC, Petersen EB, Bobst JA *et al.* Effects of direct current electrical stimulation on gene expression of osteopromotive factors in a posterolateral spinal fusion model. *Spine* 2006;**15**:174 181.
37. Roberts WE, Turley PK, Brezniak N, Fielder PJ. Bone physiology and metabolism. *J Calif Dent Assoc* 1987;**15**:54 61.

9 ANEXO

9.1 NORMAS DO PERIÓDICO *JOURNAL OF BONE AND MINERAL RESEARCH* PARA PUBLICAÇÃO

Author Guidelines

COVER IMAGES. Authors wishing to submit images for consideration for use on the front cover of the *JBMR*® are encouraged to do so. Images and questions regarding cover images should be emailed to JBMRoffice@wiley.com.

Quick Links
ARRIVE, CONSORT, STROBE, PRISMA checklists
Editorial Policies
Author rights for reuse and open access
Types of manuscripts published
Preparation and submission of manuscripts
Organization and format of manuscripts
Review process and decisions timeline
ASBMR Raisz-Drezner Journal of Bone and Mineral Research (JBMR®) First Paper Awards
Publication fees

EDITORIAL POLICIES

The *JBMR*® is a member of, and subscribes to the principles of, the **Committee on Publication Ethics (COPE) www.publicationethics.org.**

Author Agreement: The conflict of interest (COI) and copyright transfer (CTA) portions of the current Author Agreement can now be completed electronically as a web form, eliminating the need for authors to print, scan and upload a PDF form upon submission.

• COI information will be collected during submission via an online questionnaire on ScholarOne.

• The CTA will be completed at manuscript acceptance: If a manuscript is accepted for publication, the corresponding author will receive an e-mail prompt to log in to Author Services. Author Services is a Wiley web application that provides production tracking, as well as other resources for authors. From this site, corresponding authors can complete the CTA on behalf of all authors on the paper.

Copyright. The *JBMR*® is the official journal of the American Society for Bone and Mineral Research (ASBMR), which holds copyright to all material published in the Journal except as noted in the Author Agreement.

If your paper is accepted, the corresponding author will be able to complete the license agreement on behalf of all authors on the paper via the Wiley Author Licensing Service (WALS).

Employees of the US National Institutes of Health (NIH) may use the NIH Publishing Agreement in lieu of the standard author agreement *JBMR*®

Gold Open Access - OnlineOpen. The *JBMR*® offers authors an open access option called OnlineOpen, to have their article immediately freely available to everyone, including those who don't subscribe. To cover the cost of publishing OnlineOpen, authors pay an article publication charge (APC). The APC for this journal can be found on Wiley's OnlineOpen Pricing page.

Authorship and Acknowledgment of Contributors. The *JBMR*® has adopted the requirements for authorship and acknowledgment of contributors recommended by the International Committee of Medical Journal Editors (ICMJE) in the Uniform Requirements for Manuscripts Submitted to Biomedical Journals, August 2013 update.

All manuscripts submitted to the *JBMR*® must adhere to the following requirements:

• Those listed as authors must have each 1) made substantial contributions to conception and design, acquisition of data, or analysis and interpretation of data; 2) participated in drafting the manuscript or revising it critically for important intellectual content; 3) approved the final version of the submitted manuscript, and 4) agree to be accountable for all aspects of the work in ensuring that questions related to the accuracy or integrity of any part of the work are appropriately investigated and resolved.

• The respective roles of each author must be summarized in the Acknowledgments section of the manuscript.

• One or more of the authors must accept responsibility for the integrity of the data analysis and that author/those authors must be identified as such in the Acknowledgments section of the manuscript.

• All persons who have made substantial contributions to the work reported in the manuscript (e.g., data collection, analysis, writing, or editing assistance), but who do not fulfill the requirements for

authorship specified above, must be named, with their specific contributions, in the Acknowledgments section of the manuscript.

• The authors must obtain the permission of all those who are identified in the Acknowledgments section of the manuscript.

• One author will serve as the primary correspondent (corresponding author) for the manuscript; the corresponding author is responsible for transmitting the editors' comments to his or her co-authors.

• Authorship may not be modified after an article is accepted. Changes to the author list after submission must be detailed and justified in the cover letter.

Authors should note that the JBMR has adopted the following statement of policy based on a similar statement in the Information for Authors of the Annals of Internal Medicine:

Medical writers and pharmaceutical industry employees can be legitimate contributors to a manuscript. It is, however, particularly important that the roles, affiliations, and any potential conflicts of interest of all such contributors be included in the Acknowledgments section of the manuscript when it is submitted to the *JBMR*®. The editors consider that failure to acknowledge such contributors constitutes ghost authorship, which is contrary to the editorial policy of the *JBMR*®.

Disclosures/Conflicts of Interest. The *JBMR*® follows ICMJE guidelines for disclosure of potential conflicts of interest, and every paper published in the *JBMR*® includes a "Disclosures" section.

Scientific Misconduct. If an author violates any of the Journal's policies described above, the editors may reject the manuscript, impose a moratorium on the consideration of new manuscripts from the authors, issue a statement of concern, or retract an already-published article. In addition, the editors may contact the Office of Research Integrity and/or an official at the authors' home institution.

Duplicate/Redundant Publication. The corresponding author is responsible for ensuring that the manuscript — including all data, figures, tables, and supplementary materials — has not been previously reported or published. Further, it is the responsibility of the corresponding author to ensure that the manuscript has not been, and will not be, submitted to another journal while under review by the *JBMR*®. Original Articles providing new data from studies that have been the subject of previous publications must avoid overlap in the data reporting and authors must provide information on all relevant publications in their cover letter to the Editor-in-Chief.

Plagiarism and Image Integrity. The *JBMR*® utilizes Ithenticate to check submitted manuscripts to ensure that the text has not been plagiarized. Figures will also be scrutinized by the editors to ensure that images have not been inappropriately manipulated.

Clinical Trials. Clinical Trials submitted for publication in the *JBMR*® must conform to the Principles for Protecting Integrity in the Conduct and Reporting of Clinical Trials published by the American Association of Medical Colleges (AAMC). Authors should carefully read the AAMC Principles to ensure that their manuscripts are in full compliance, noting in particular the following:

•Authors of Clinical Trial manuscripts must indicate, in the cover letter, whether the study has conformed to a pre-specified analysis.

•Authors of Clinical Trial manuscripts must agree to provide the protocol and pre-specified analysis plan, along with amendments to and deviations from the plan, if requested by the *JBMR*® editors.

•Trial registration must include the minimum amount of trial information as defined by the World Health Organization (WHO) Trial Registration Data Set (see www.who.int/ictrp/network/trds/en/index.html).

Human Subjects/Declaration of Helsinki. Research carried out with human subjects must comply with the World Medical Association Declaration of Helsinki — Ethical Principles for Medical Research Involving Human Subjects. A statement to this effect must appear in the Methods section of the manuscript, including the name of the body that gave approval. Identifying information of human subjects within written descriptions, photographs, or pedigrees should not be published. Additionally, clinical research studies must be registered with the appropriate national body (see www.wma.net/en/30publications/10policies/b3/17c.pdf).

STROBE: Authors of manuscripts reporting results of human observational case-control, cohort, or cross-sectional studies are required to upload the STROBE (STrengthening the Reporting of OBservational studies in Epidemiology) checklist at submission.

Use of Animals in Research. To be considered for publication in the *JBMR*®, research carried out on animals must be in compliance with the guiding principles in the Guide for the Care and Use of Laboratory Animals: Eighth Edition, ISBN-10: 0-309-15396-4. Approval by the appropriate institutional animal care and oversight committee must be indicated in the Methods, along with full husbandry and experimental details (e.g. strain, sex, replicate number, the method used to calculate

the sample size and power of analysis) as indicated by the Animal Research Reporting of In Vivo Experiments (ARRIVE) checklist.

ARRIVE: Authors submitting research on animal studies are required to complete an adapted ARRIVE Animals in Research: Reporting In Vivo Experiments checklist with their submission.

CONSORT: Authors of manuscripts reporting results of clinical trials are required to upload the CONSORT (Consolidated Standards of Reporting Trials) checklist with their submission.

PRISMA: Authors of manuscripts reporting results of systematic reviews and meta-analyses are required to upload the PRISMA Preferred Reporting Items for Systematic Reviews and Meta-Analyseschecklist with their submission.

While publication of **Human Genetic Study** discoveries is a central element for disseminating knowledge, the Journal's responsibility is to ensure that the design, analysis, and interpretation of the results of human genetic studies published in the Journal meet key aspects of scientific rigor similar to those stipulated by the STrengthening the REporting of Genetic Associations (STREGA) statement. Please click here to read the full guidelines on Human Genetic Studies.

Availability/Disclosure of Materials and Methods and Author Access to Data. Authors of papers submitted to the *JBMR*® must make materials and methods (e.g., cell lines, hybridomas, DNA clones, antibodies, biological reagents, and animal models) described in articles published in the *JBMR*®available to scientists in non-commercial institutions for purposes of replicating reported studies. Additionally, any original nucleotide/amino acid sequence data presented in a manuscript must be submitted to GenBank www.ncbi.nlm.nih.gov/genbank by the authors, and the accession numbers must be included with the submitted manuscript.

Encourages Data Sharing

Wiley and the ASBMR support efforts to encourage the sharing of research data. Journals and publishers are in a position to make a significant contribution to enabling access to the data underlying the articles we publish. The sharing of data enables others to reuse experimental results and supports the creation of new work built on previous findings, improving the efficiencies of the research process and supporting the critical goals of transparency and reproducibility. The policies concern the research data that support the results documented in research articles, including but not limited to: raw data, processed data, software, algorithms, protocols, methods, materials.

The ASBMR journals encourage authors to share the data and other artifacts supporting the results in the paper by archiving it in an appropriate public repository. Authors should include a data accessibility statement, including a link to the repository they have used, in order that this statement can be published alongside their paper.

There are many options for depositing and sharing research data. One available repository is Figshare, which is integrated with the Wiley platform within existing journal workflows. Information on Data Sharing and Figshare can be found here: https://authorservices.wiley.com/author-resources/Journal-Authors/licensing-open-access/open-access/data-sharing.html. Do not hesitate to contact the editorial office at *JBMR*® Editorial Office for more information on Figshare or other supported depositories.

AUTHOR RIGHTS FOR REUSE AND OPEN ACCESS

Preprint Use

Preprint servers, i.e., servers that allow for the posting of papers prior to submission for publication, are becoming more common across a range of disciplines. We know that preprint servers are far from ubiquitous and that their use is not universally accepted, but preprints are an important topic of conversation in many research communities.

This journal will consider for review manuscripts previously available as preprints on non-commercial servers such as ArXiv, bioRxiv, psyArXiv, engrXiv, etc. The manuscript cannot be under consideration by another journal at any time that it is under consideration by *JBMR*® . Authors may also post the submitted version of their manuscript to non-commercial servers at any time. Authors are requested to update any pre-publication versions with a link to the final published article.

Self-archiving Policy

Authors may self-archive the peer-reviewed (but not final) version of their paper on their own personal website, in their company/institutional repository or archive, and in not-for-profit subject-based repositories such as PubMed Central, following an embargo period of 12 months for scientific, technical, or medical journals. The version posted may not be updated or replaced with the VoR (Version of Record, which is the final, published version) and must contain the text, "This is the accepted version of the following article: [FULL CITE], which has been published in final form at [Link to final article]."

Funder Arrangements and Article Repositories

Certain funders, including the NIH, members of the Research Councils UK (RCUK), and Wellcome Trust require deposit of the Accepted Version in a repository after an embargo period. Details of funding arrangements are set out at the following website www.wiley.com/go/funderstatement. Please contact the Journal production editor if you have additional funding requirements.

The *JBMR*® supports its authors by depositing the accepted version of articles by National Institutes of Health (NIH) grant-holders to PubMed Central upon acceptance by the journal. Authors must first indicate during the submission process that their work was funded by the NIH.

1. Wiley (as publisher of *JBMR*®) automatically deposits the accepted version to PubMed Central (PMC) 2 to 4 weeks after manuscript acceptance.

The accepted version is the version that incorporates all amendments made during peer review, but prior to the publisher's copy editing and typesetting.

2. PMC issues an NIHSMID number and sends an email to the corresponding author to approve submission. The corresponding author's approval is a critical step in the process.

3. Three months after publication of the version of record (VoR), PMC issues the PMCID.

The VoR is the definitive published version of the article that appears in a paginated issue. The VoR has had value added by the publisher such as copyediting, formatting, etc. to become a living part of the scholarly record.

4. Twelve months after publication of the VoR, the accepted version appears in PubMed Central.

The NIH mandate applies to all articles based on research that has been wholly or partially funded by the NIH and that are accepted for publication on or after April 7, 2008.

NIH authors may also choose the OnlineOpen service as another option for NIH compliance. Upon payment of the OnlineOpen article publication charge ($3,000), Wiley will deposit the VoR into PubMed Central, with public availability in PubMed Central and the JBMR® website immediately upon publication.

OnlineOpen

OnlineOpen fulfills RCUK, Wellcome Trust, NIH, FWF, Telethon Italy, and other funder mandates. With OnlineOpen, the author, the author's funding agency, or the author's institution pays a fee to ensure that the article is open access and freely available to all on

Wiley Online Library. In addition, authors of OnlineOpen articles are permitted to post the final, published PDF of their article on a website, institutional repository or other free public server, immediately on publication. For the full list of terms and conditions, see: http://olabout.wiley.com/WileyCDA/Section/id-406241.html.

The fee for OnlineOpen in *JBMR*® is $3,000 US. OnlineOpen is activated upon payment and can be ordered at any point prior to, or after, acceptance. To make your article OnlineOpen, please complete the OnlineOpen Form.

For Authors Choosing OnlineOpen

If your paper is accepted, the author whom you identify as being the corresponding author for the paper will be presented with the option to sign an open access agreement (on behalf of all co-authors) to make the article available under the terms of the Creative Commons Attribution-Non-Commercial-NoDerivatives (CC-BY-NC-ND) license. For more information on the terms and conditions of the license please visit:

http://www.wileyopenaccess.com/details/content/12f25db4c87/Copyright--License.html

The open access agreement is administered electronically. The author identified as the formal corresponding author for the paper will receive an email prompting them to login into Author Services; where via the Wiley Author Licensing Service (WALS) they will be able to complete the license agreement on behalf of all authors on the paper.

If you select the OnlineOpen option and your research is funded by The Wellcome Trust and members of the Research Councils UK (RCUK), you will be given the opportunity to publish your article under a Creative Commons Attribution License OAA (CC-BY) license, which supports you in complying with Wellcome Trust and Research Councils UK requirements. For more information on this policy and the Journal's compliant self-archiving policy, please visit:http://www.wiley.com/go/funderstatement and the "Creative Commons Attribution License"section posted on http://www.wileyopenaccess.com/details/content/12f25db4c87/Copyright--License.html.

TYPES OF MANUSCRIPTS PUBLISHED

In order to consolidate and simplify the type of manuscripts that the journal will hence forth publish, below please find the accepted article types. Please see a recent Editorial by the JBMR® Editorial team Focusing on the Science - *JBMR*® Manuscript Types.

Original Articles. Original Articles should be kept to within approximately 28 double-spaced pages of 12-point Times Roman text, including the text of the manuscript, references, figures, figure legends, tables, and table footnotes.

Clinical Trials. Manuscripts reporting clinical trials should be kept to within approximately 28 double-spaced pages of 12-point Times Roman text, including the text of the manuscript, references, figures, figure legends, tables, and table footnotes.

Letters to the Editor. The *JBMR*® welcomes Letters to the Editor that contribute constructively and substantively to scientific dialogue. Letters should address timely and important issues raised in articles recently published in the *JBMR*® and should be no more than 900 words. Note that the *JBMR*®only considers Letters to the Editor that comment on papers previously published in the Journal and letters may not contain unpublished data.

Reviews and Mini-Reviews (Perspectives). The *JBMR*® publishes Reviews and Perspectives (Mini-Reviews) on topics selected by the editors. Reviews are approximately 6,000 words in length and Perspectives are approximately 2,800 words. Authors should not submit Reviews or Perspectives without first contacting the *JBMR*® Editorial Office.

Editorials (formerly called Commentaries). Editorials can be short articles written by the editors to provide information about the journal and its policies. The Editorial format is also now used to highlight an article judged of particular impact and relevance. Editorials are invited by the editors and unsolicited Editorials are rarely published. Authors should not submit Editorials without first contacting the *JBMR*® Editorial Office.

PREPARATION AND SUBMISSION OF MANUSCRIPTS

This section presents detailed instructions on how to prepare and submit a manuscript to the *JBMR*®. Questions may be addressed to the *JBMR*® Editorial Office. Manuscripts that do not conform to the *JBMR*®'s policies or requirements, including requirements for manuscript organization, format, and figure and image size and quality will be returned to the authors without review.

Manuscript Submission. Manuscripts must be submitted to the *JBMR*® via the Journal's online submission system by a single corresponding author at https://mc.manuscriptcentral.com/asbmr. Only the designated corresponding author will be able to view the submission's status or make changes to the manuscript. If you change the corresponding author during submission, the manuscript will be

removed from your account and placed into theirs. There can be only one corresponding author per manuscript.

Authors are now required to provide both a clean and marked-up version of each revision.

Questions about manuscript submissions should be directed to the *JBMR*® Editorial Office, jbmroffice@wiley.com.

JBMR® asks authors to classify their manuscript at the time of submission as Basic, Clinical, or Translational:

• Basic: a study limited to in vitro studies of cell biology, molecular biology, etc.

• Clinical: a study with the major component of the work involving human subjects

• Translational: any study involving predominantly animal models or where the laboratory and clinical aspects of a human study are of approximately equal weight.

Manuscript Details. Your manuscript may be submitted as a PDF file with figures and tables embedded at original submission. We will require that all files used to create the PDF, including figures, be submitted separately when a revision is requested. All manuscript pages must be numbered consecutively in the bottom right-hand corner, including references, tables, and figure legends.

Should a revision be requested, you will be required to upload your manuscript and table(s) in .doc/.docx format, and figures will be required to be uploaded separately as .tif or .eps files.

English-language Services. If you are not a native English speaker, Wiley Editing Services provides resources to help improve the English of your paper before submission.

Authors in Japan may visit Wiley-Japan for additional resources and information at http://www.wiley.co.jp/journals/editcontribute.html.

Authors in China are encouraged to visit Wiley-China at http://www.wiley.com/WileyCDA/Section/id-WILEYCHINA.html.

Nomenclature. Abbreviations and nomenclature must follow the recommendations of the International Union of Biochemistry. Use of the International System of Units (SI units) is required; include appropriate conversion factors to aid the reader where appropriate. Drug names should always be generic.

Papers on or that make use of bone histomorphometry must use the nomenclature, symbols, and units as described at Dempster et al.

Papers that include micro–computed tomography (?CT)-derived bone morphometry and density measurements in animal models must

cite and use the nomenclature, symbols, and units as described in Bouxsein et al.

Papers on the descriptive epidemiology of osteoporosis should, wherever possible, include bone mineral density measurements made at the femoral neck and should report T-scores or diagnostic categories derived from standardized measurements using the NHANES III reference base for Caucasian women.

Abbreviations and Acronyms. Nonstandard abbreviations must be spelled out at first mention, with the abbreviated form appearing in parentheses. Thereafter, they should be used without definition. Standard *JBMR*® abbreviations do not need to be defined.

ORGANIZATION AND FORMAT OF MANUSCRIPTS

The order of manuscript elements is as follows:

- Cover Letter
- Title Page
- Disclosure Page
- Abstracts
- Introduction
- Materials and Methods
- Results
- Discussion
- Acknowledgments
- References
- Figure Legends
- Tables
- Figures
- Supplemental Data

Descriptions of each manuscript element are provided below.

Cover Letter. The cover letter should briefly outline the major findings of the study and the potential significance of these findings in the fields of bone and mineral research. Additionally, the authors may elect to indicate suggested reviewers in their letter, along with any reviewers to whom they might be opposed.

Title Page. The title page must include the title, names of the authors (in the same order as the manuscript) and their major degrees, and affiliations and grant supporters.

The corresponding author's address, telephone number, and email address must also be provided. Finally, this page must indicate if any supplemental data have been included with the submission.

Important: All those listed as authors must meet the requirements specified in the "Authorship" section under "Editorial Policies," above. All those who qualify for authorship must be listed.

Disclosure Page. Disclosures must be included at the time the manuscript is initially submitted to the *JBMR*®. *JBMR*® follows ICMJE requirements, and authors will be required to sign and fill out a disclosure eform, which incorporates the ICMJE requirements at the time of submission.

Title. **The title is the most important criterion for search engines and PubMed.** The title must be concise and should accurately reflect the scope of the study, including the species investigated. Editors reserve the right to edit titles that are not clear and succinct. In order to create a search engine friendly title, we suggest you follow these guidelines:

- Include 1-2 keywords related to your topic
- Place your keywords within the first 65 characters of your title
- Keep your title short
- Consider moving a phrase from your title to the first or second sentence of your abstract
- Mention species in which study is conducted
- Should attract attention of the reader

Abstract. An abstract that briefly summarizes the major findings of the study must be included. It must be unstructured (i.e., there should not be introduction, methods, results sections, etc.), self-explanatory (i.e., completely understandable without reference to the text of the manuscript), and must not exceed 300 words. Five key words should be listed at the bottom of the Abstract page. Click here for a full list of key words.

Introduction. This section should concisely review the rationale for the study and identify what issues are to be addressed. Background information directly pertaining to and necessary for the understanding of the study should also be included. This should clearly place the article within the area being studied and should not describe the outcome of the study in any detail.

Materials and Methods. This section should carefully describe the methods and materials used, including statistical approaches (see below). It is not necessary to describe commonly used techniques in detail. Experiments must be outlined in sufficient detail to enable repetition by others, including the sequence and source of unique constructs. Any limitation of authors to full data access (e.g., blinded,

etc.) must be explained. Restrictions on access to materials or experimental animals should be specified (for details, see "Use of Animals in Research" and“Availability/Disclosure of Materials and Methods and Author Access to Data”).

Results.This section should succinctly state the results without lengthy discussion or interpretation of individual data. Graphical format is often preferable to tabular presentation of data.

Statistical Analysis. Authors are responsible for ensuring that data presented in a manuscript are reproducible and that any differences in these data, upon which the authors draw conclusions, are not merely the result of random variation, (i.e., are statistically significant). Statistically significant findings are not prerequisites for publication in the *JBMR*®; however, properly analyzed data indicating null association or null effect can also be highly informative and publishable.

Since statistical analyses vary according to study design and prohibit the establishment of standard rules, guidelines are available here to assist authors in performing the most appropriate statistical analyses and reporting those results in accord with *JBMR*® standards.

Discussion. Study results should be summarized, though not repeated in detail, to provide context for logical explanations of the reported results and extrapolations or hypotheses drawn from them. The Discussion should conclude by re-stating the major findings of the study in relation to the rationale and aims of the study as outlined in the introduction. A concluding remark regarding wider implications of study findings is expected.

Acknowledgments. Authors must acknowledge all support for the work, including funding, materials, equipment, drugs, technical assistance, etc. Acknowledgments should conform to the requirements detailed in the “Editorial Policies/Authorship and Acknowledgment of Contributors”section.

In addition, the *JBMR*® requires that each author briefly summarize his or her respective role. Example:

Authors’ roles: Study design: TC and DD. Study conduct: RF. Data collection: AF. Data analysis: RF and AF. Data interpretation: TC, DD, RF, and AF. Drafting manuscript: TC and DD. Revising manuscript content: RF, and AF. Approving final version of manuscript: TC, DD, RF, and AF. RF takes responsibility for the integrity of the data analysis.

References. Authors are responsible for the accuracy of their references. References must be numbered consecutively in the order they appear in the text. Place each reference number in parentheses,

throughout the text, tables, and legends. Use parentheses, as in this example (1). If the same reference is used again, re-use the original number.

Please click here to view our Reference Style Sheet.

Figure Legends. A separate list of figure legends must be supplied at the end of the manuscript. These should provide sufficient information for the figure to be understood independent of the text. Do not include these legends in the figure files themselves.

Tables. Tables should complement the text without reiterating it. Tables should be numbered consecutively according to the order in which they are cited in text. Each table should have a brief, descriptive title. All necessary information should be contained in the footnote, and the table itself must be understandable independent of the text. Tables should not contain color. Provide each table column with an appropriate heading, and indicate clearly any units of measurement in the table. A key should be provided in the footnote for any symbols used. Tables may be embedded into the manuscript DOC or DOCX file. Superscript notation using sequential letters to indicate statistical significance (e.g., 342 ± 14a) is preferable to the use of non-sequential symbols.

Figures. Figures should be labeled with Arabic numerals (Figure 1, 2, etc.) and panels labeled with letters (A, B, C). The *JBMR*® allows the use of videos as primary figures; in order to do so, you must submit a screen capture from the video for use in the printed version of the Journal. The y-axis of graphs should originate at 0 or should show a clear scale break in cases where this would be difficult.

Figures should be sized to one-column width (20 picas, 84 mm), or two-column width (42 picas, 177 mm), as appropriate. Multi-panel images should be composed as a single image with width and height limitations applying to the final, combined image. Image resolution must be at least 300 dpi for raster images (e.g., photographs, gels, stains) and 600 dpi for line-art images (e.g., charts and graphs). Image-related text and labeling must be clearly legible in a font size of 10 points or greater Times New Roman in the final image.

Images presented in figures must adhere to the Guidelines for Best Practices in Image Processing: http://ori.hhs.gov/education/products/RIandImages/guidelines/list.html.

Figures should not include figure legends. Figures must be submitted in TIF or EPS formats. The *JBMR*®cannot accept figures in PDF, PPT, or PPTX formats because the quality of print reproduction of figures in these formats is poor. For further guidance on preparing

digital figure files, author(s) are encouraged to visit http://cjs.cadmus.com/da/applications.asp.

Supplemental material. Supplemental material may be submitted to accompany an article for online-only publication when there is insufficient space or it is not possible to include the material in print. Supplemental materials will also be reviewed and controlled for plagiarism and falsification.

Supplemental material must be uploaded separately from the manuscript and figures. Unless specifically requested by the editors during the review process, supplemental material must be submitted along with the manuscript and not after the peer review process has begun or has been completed. The *JBMR*® will not accept supplemental material after an article has been accepted. Supplemental figures and tables must be referenced in the manuscript and appropriately labeled, i.e., "Supplemental Figure 1," "Supplemental Figure 2," etc.

Although the *JBMR*® does not set strict limits on the amount of supplemental material, authors should make efforts to keep the amount of such material to a reasonable level and submit only what is necessary to improve the communication of the paper's key scientific points.

Please note that supplemental information will be subjected to the full review process, but will not be checked for typographical errors or technical functionality. The responsibility for such errors and file functionality remains entirely with the authors. A disclaimer will be displayed to this effect with any supplemental information published. Questions about missing supporting information on Wiley Online Library should be directed to the journal's production editor.

Wiley does not provide technical support for the creation of supporting information. For more information, please see http://authorservices.wiley.com/bauthor.

REVIEW PROCESS AND DECISIONS TIMELINE

The *JBMR*® receives more than 800 submissions annually and must therefore be highly selective. The editors typically accept no more than around 25% of the manuscripts submitted each year. Manuscripts that the editors judge unlikely to be accepted may be returned to the authors without peer review. After acceptance, the time to online publication of the non-copyedited "Accepted Article" version of a paper is typically two weeks.

Author Services enables authors to track their article - once it has been accepted - through the production process to publication online and in print. Authors can check the status of their articles online and choose to receive automated e-mails at key stages of production. The author

will receive an e-mail with a unique link that enables them to register and have their article automatically added to the system. Please ensure that a complete e-mail address is provided when submitting the manuscript. Visit http://authorservices.wiley.com/bauthor for more details on online production tracking and for a wealth of resources including FAQs and tips on article preparation, submission and more.

Once your article is published, Wiley offers a variety of tools to help you track impact and manage publicity. Please see the Author Toolkit for more information.

ASBMR RAISZ-DREZNER JOURNAL OF BONE AND MINERAL RESEARCH (JBMR®) FIRST PAPER AWARDS

Lawrence G. Raisz, M.D. founded the Journal of Bone and Mineral Research (JBMR®)and served as Editor-in-Chief for the first 10 years of the journal's existence. Under his leadership, the JBMR® expanded from a bimonthly to a monthly publication, began publishing the best science in bone and mineral metabolism and emerged as the highest-ranked journal in its field. Marc K. Drezner, M.D., built upon Dr. Raisz' success by maintaining the Journal's #1 ranking, expanding its international reach, instituting self-publishing and establishing a fully electronic presence for the journal.

The ASBMR Raisz-Drezner Journal of Bone and Mineral Research(JBMR®) First Paper Awards honor first authors of meritorious scientific publications published in the JBMR®. To qualify for consideration, a paper must be the first JBMR® scientific paper in which the first author appears as first author. Among qualifying submissions that reach final acceptance, one such paper will be determined by the review committee to be of highest merit. The award includes a $1,000 honorarium and a plaque, both of which are presented to the recipient at the ASBMR Annual Meeting.

Eligibility

To qualify for consideration for the ASBMR Raisz-Drezner Award in 2018, a paper must:

• Be the first JBMR® scientific paper where the first author appears as first author
• Have been submitted between July 1, 2017 and May 31, 2018

Papers accepted for publication in the JBMR® that were submitted according to the eligibility guidelines noted above will be submitted to the review committee. No additional application is required.

PUBLICATION FEES

Submission Fee. The *JBMR*® charges a fee of $50.00 US for all unsolicited submissions with the exception of revised manuscripts, invited Reviews and Commentaries, and Letters to the Editor. Please click here to access the online Manuscript Submission Fee Form.

ASBMR can no longer accept faxed or emailed credit card payments. To pay your manuscript submission fee with credit card, please visit the ASBMR website. To pay with check or to request an invoice, please email asbmr@asbmr.org.

Publication fees. Effective from September 1, 2016, the Journal of Bone and Mineral Research (JBMR®) color page-fee charges will be replaced with a flat fee. ASBMR members will pay $1,200 USD and non-ASBMR members will pay $1,800 USD per published manuscript, which includes unlimited color images. All other charges will remain the same, including the manuscript submission fee of $50 USD, and the open access online open fee of $3,000 USD. Invited material is not subject to article publication charges.